AMERICAN UNIVERSITY OF BEIRUT

BOLTZMANN MODEL FOR THE LATTICE THERMAL CONDUCTIVITY IN SEMICONDUCTOR NANOWIRES

by
DINA MERHEJ THEBIAN

A thesis
submitted in partial fulfillment of the requirements
for the degree of Master of Science
to the Department of Physics
of the Faculty of Arts and Sciences
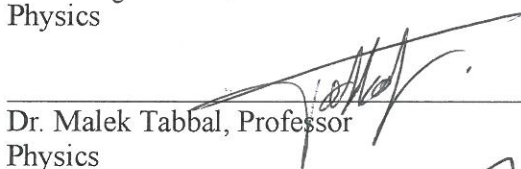at the American University of Beirut

Beirut, Lebanon
February 7 2017

AMERICAN UNIVERSITY OF BEIRUT

BOLTZMANN MODEL FOR THE LATTICE THERMAL CONDUCTIVITY IN SEMICONDUCTOR NANOWIRES

by
DINA MERHEJ THEBIAN

Approved by:

_____

Dr. Michel Kazan, Associate Professor   Advisor
Physics

_____

Dr. Malek Tabbal, Professor   Committee Member
Physics

_____

Dr. Mazen Ghoul, Professor   Committee Member
Chemistry

Date of thesis defense: February, 7, 2017

AMERICAN UNIVERSITY OF BEIRUT

THESIS, DISSERTATION, PROJECT RELEASE FORM

Student Name:

_____Thebian_____Dina_____Merhej_____

                        Last   First   Middle

☑ Master's Thesis   ◯ Master's Project   ◯ Doctoral
Dissertation

☑   I authorize the American University of Beirut to: (a) reproduce hard or electronic copies of my thesis, dissertation, or project; (b) include such copies in the archives and digital repositories of the University; and (c) make freely available such copies to third parties for research or educational purposes.

☐   I authorize the American University of Beirut, to: (a) reproduce hard or electronic copies of it; (b) include such copies in the archives and digital repositories of the University; and (c) make freely available such copies to third parties for research or educational purposes
after : **One ----**   **year from the date of submission of my thesis, dissertation, or project.**
       Two ----   **years from the date of submission of my thesis, dissertation, or project.**
       Three ---- years from the date of submission of my thesis, dissertation, or project.

_Dina Thebian_____   _2/8/2017_____

Signature   Date

ACKNOWLEDGMENTS

First and foremost, I would like to thank my advisor, Dr. Michel Kazan, for his help and guidance throughout the thesis. I would like to express my gratitude to him for his continuous support, valuable advices and encouragement. It has been an honor working with such a motivated researcher with immense knowledge.

I would like to express my deepest thanks to my thesis honorable committee members, Dr. Malek Tabbal and Dr. Mazen Al Ghoul. I really appreciate your support, thoughtful advices and time. I am grateful for everything you have taught me.

Special thanks go to all my professors who taught me throughout my graduate studies.

I am thankful for my amazing partner for his unconditional support and understanding. To my loving parents, I am grateful for your warm encouragement and endless support. Deepest appreciation goes to all my family members.

AN ABSTRACT OF THE THESIS OF

Dina Merhej Thebian   for   Master of Science
                              Major: Physics

Title: Boltzmann Model for the Lattice Thermal Conductivity in Semiconductor
       Nanowires

In this thesis, we have developed a theoretical model to predict the thermal conductivity for cylindrical and pristine nanowires. Boltzmann equation is solved including spatial dependence of the phonon distribution function and taking into account all the phonon scattering mechanisms and the differences in their physical nature.

Vibrational parameters such as Debye temperature and Grüneisen parameter are derived as a function of temperature and crystallographic directions using the lattice dynamics approach to be employed in the calculation of the lattice thermal conductivity. Houston's method is used for the calculation of the phonon spectrum, which will be involved further in the general formalism of the lattice thermal conductivity.

In an attempt to draw an understanding of the effects of the size and surface on the lattice thermal conductivity, we have studied the effect of the scattering of the phonons by the boundaries of a nanowire with a circular cross section. Expression for the boundary scattering relaxation time of phonons in the presence of other anharmonic phonon scattering mechanisms are developed. The intrinsic phonon scattering rates are calculated from Fermi's Golden Rule.

With this presented model, the lattice thermal conductivity for cylindrical and pristine nanowires can be calculated. This model shows the different behavior of the lattice thermal conductivity for nanowires, in comparison to bulk, demonstrated with reference to experimental measurements.

CONTENTS

V. THERMAL CONDUCTIVITY OF CYLINDRICAL NANOWIRES 50

CHAPTER I

INTRODUCTION

As the size of devices and structures has become smaller and smaller and entered the nanoscale, the physical principles governing their operation are changing dramatically [1]. Studying heat transfer in nanostructures has been of great interest to physicists and engineers for its high importance in many nanotechnology applications. With device or structure characteristic length scales becoming comparable to the mean free path and wavelength of heat carriers (electrons, photons, phonons, and molecules), classical laws are no longer valid [2]. While electrons are the major thermal and charge carriers in metals, phonons (i.e., atomic vibrations) dominate the thermal transport in crystalline semiconductors [3]. Heat transfer in nanostructures differs from their bulk counterparts. For example, thermal conductivity is no longer a material property at the nanoscale. Studies on thermal conductivity of materials and its management have been of great interest in the past years because of its technological importance. There are typically two types of problems. One is the management of heat generated in nanoscale devices to maintain the functionality of these devices and the other is to utilize nanostructures to manipulate the heat flow and energy conversion [4]. Examples of the thermal management of nanodevices are the heating issues in integrated circuits [5] and in semiconductor lasers [6]. Example in the manipulation of heat flow and energy conversion includes nanostructures for thermoelectric energy conversion [7, 8]. Correspondingly, high thermal conductivity materials are used in heat sink applications

1

and low thermal conductivity materials are needed for thermal insulation and power generation through thermoelectric conversion.

Studying heat transfer in solids requires an understanding of lattice vibrations. Atoms in solids are packed closely with a harmonic potential between them. They are not quite stationary but oscillate around their equilibrium positions giving rise to a set of vibrational propagating waves through the lattice. The interatomic forces bond nuclei together so that the vibration of the atoms inside the crystal is strongly coupled [1]. The picture can be visualized as a set of coupled harmonic oscillators where the lattice has a standing wave like solution upon solving equations of atomic motion. The atomic vibration can be decomposed into normal modes extending over the crystal and the basic energy quanta of each normal mode is called a phonon [1]. In other words, a phonon wave function is characterized by a vibrational frequency (energy) and a wave vector that corresponds to a single normal mode of the lattice vibration. The dependence of the phonon frequency on the wave vector is known as the dispersion relation. We have two types of phonons; acoustic and optical. Acoustic phonons are the main carriers of heat because of their high group velocity and they describe the coherent oscillations of atoms around their specific lattice sites. Acoustic phonons are low frequency phonons and exhibit a linear dispersion relation for long wavelengths. While optical phonons, out-of-phase movements of atoms, belong to the high frequency branch. In fact, due to their low group velocity optical phonons cannot contribute significantly to heat, so they decay into acoustic ones and affect the lattice thermal conductivity as was shown in nanowires.

The general approach in calculating the thermal conductivity of materials in which heat is carried by phonons is to solve the Boltzmann equation under the

relaxation time approximation in which the scattering cross section is calculated by perturbation techniques. Boltzmann equation describes the statistical behavior of a system in a non-equilibrium state. The latter states the total rate of change of the phonon distribution function from equilibrium in the presence of temperature gradient and phonon scattering mechanisms.

The behavior of the lattice thermal conductivity is early described by Debye and Peierls and is in good agreement with experiment. At very low temperatures the thermal conductivity depends on the size and shape of the crystals and increases with the temperature modeling the behavior of the specific heat (T^3 dependence). The thermal conductivity reaches a peak where it is sensitive to imperfections such as impurities and defects and then starts to drop at temperatures above $0.1\Theta_D$ at which phonon umklapp scattering processes dominate. Following the early work of Debye and Peierls, several models have been proposed to calculate the lattice thermal conductivity. In 1959 Callaway developed a phenomenological model to calculate the lattice thermal conductivity at low temperatures. He assumed an isotropic, Debye-like phonon spectrum. He made no distinction between longitudinal and transverse phonons and the phonon branches are non-dispersive. Callaway represented the phonon scattering processes by frequency-dependent relaxation times. He assumed four scattering processes: (1) normal three phonon processes, (2) umklapp processes, (3) point impurities (isotope), and (4) boundary scattering. Three phonon normal processes for which Callaway assumed a relaxation time that goes like $(B_2 \, \omega^2 \, T^3)^{-1}$ where B_2 is a parameter that depends on Gr$\ddot{u}$neisen constant and the phonon velocity. Umklapp mechanism for which the relaxation time has an exponentially decaying behavior $\exp(\Theta_D/bT)$ at high temperature. The isotope scattering takes an independent

temperature form $(\omega^4)^{-1}$. With respect to the boundary scattering, Callaway assumed a constant relaxation time L/c where L is the characteristic length of the sample and c is the average speed of sound in the crystal. Callaway distinguished between normal and resistive processes. Normal processes which conserve the total crystal momentum lead to a displaced Planck distribution, while resistive processes including umklapp scattering, impurity scattering and boundary scattering tend to return the phonon system to an equilibrium Planck distribution [9]. Through some assumptions, Callaway presented an integral expression of two terms k_1 and k_2 of the lattice thermal conductivity that pertains to longitudinal modes. k_2 is considered an additional correction term to explain errors due to treating the normal processes as resistive ones and is usually neglected. The model predicts for germanium a thermal conductivity in the temperature range 50° -100°K. The results are in good agreement with experimental data but fails at the maximum of the curve. Therefore, the model is suitable for thermal conductivity only at low temperatures where the phonon spectrum is non-dispersive Debye-like and only the isotope and boundary scattering dominate.

Following the work of Callaway, Holland presented an analysis of thermal conductivity in which he considered the contribution of both longitudinal and transverse phonons to heat conduction under the assumption $k_2=0$. The scattering rates of isotope and boundary scattering mechanisms in the Holland model are the same as in the Callaway model, except that the boundary scattering is partially diffusive. In his model, Holland attempted to describe the lattice thermal conductivity behavior at high temperatures and he modified the normal and umklapp scattering relaxation times. Normal processes relaxation time corresponding to longitudinal phonons has the same Callaway form $(B_L \, \omega^2 \, T^3)^{-1}$ while the transverse modes relaxation time goes like $(B_T \, \omega$

$T^4)^{-1}$. Note that, according to Callaway model only longitudinal acoustic phonons are taken into account in the normal processes. With respect to umklapp scattering, the Holland model considers only the transverse modes and divides the term into high frequency phonon region and low frequency one. For low-frequency transverse modes, $\omega < \omega_1$, the umklapp process is absent. Transverse modes with frequencies between ω_1 and ω_2 have a relaxation time that goes like $\sim \omega$. The frequency at which U processes start is ω_1 and ω_2 is the highest transverse mode frequency [10]. With this approach, a good representation of the thermal conductivity of silicon and germanium at high temperatures is obtained.

The fact that it is unreasonable to suppress the k_2 term in Callaway's model when normal scattering processes are included [11] is studied by Asen-Palmer et al. who presented a study on the thermal conductivity of germanium crystals with different isotopic compositions. The thermal conductivity measurements were made and experimental data was analyzed according to three models: Callaway's model, Holland's theory, and a modified Callaway/Holland model. In the framework of Callaway's model, it was found that k_2 is not only a correction term to k_1 and its value is controlled by the concentration of defects and impurities. The calculations show that k_2 contributes by 20% to the total thermal conductivity in the case of pure 70Ge (99.99%) [11]. In other words, in highly defected samples where resistive processes dominate, only the k_1 term is essential. However, in isotopically pure samples where the normal processes are of importance, the k_2 term contributes significantly to the lattice thermal conductivity. A representation of the all the data was obtained below 30K using the full Callaway model. Applying Holland's theory, an acceptable representation of the thermal conductivity of the samples under study is obtained for temperatures less than

200K using a set of fitting parameters. Asen-Palmer et al. presented a modification to the above models and replaced them with the modified Callaway/Holland model. The model keeps both terms k_1 and k_2 with a distinction between transverse and longitudinal phonons. An additional relaxation time corresponding to longitudinal umklapp processes is required for which the latter is responsible for the decay of the thermal conductivity at higher temperatures. Note that Holland neglected the longitudinal U processes in his model as he expected them not to hold at high temperatures. Dividing the transverse branch into two frequency regions is no more needed and the corresponding relaxation time is modified to have an exponential dependence rather than a hyperbolic sine term. The Callaway/Holland formalism provides analysis of the thermal conductivity of Ge samples with different isotopic compositions that fits the experimental data below 200K.

Later on studies have been made by Morelli et al. on estimating the isotope effect in Ge, Si, and diamond on the lattice thermal conductivity [12]. The authors have applied the Callaway/Holland model but using more simplified phonon relaxation times. In this approach, the parameters are calculated from phonon dispersion relations of the studied crystals and are dependent on crystal properties such as Debye temperature, phonon velocities, volume and mass of the crystal, size of the sample and adjustable Grüneisen parameters. The model fits the experimental data of the thermal conductivity for silicon, germanium, diamond and silicon carbide in a wider temperature range. Note here that taking the Grüneisen parameter as a temperature-independent parameter seems physically unreasonable despite that it simplifies the calculations. Similarly, a constant Debye temperature is only reasonable at very low temperatures where the Debye theory

6

is still applicable. Thus, adopting a temperature-dependent Debye temperature widens the temperature range of the applied model as proved by previous experiments [13].

In the discussed models, the boundary relaxation time is set to a constant value which depends on the phonon velocity and the characteristic length of the sample. However, when studying crystalline solids in the nanometer range, phonon transport is controlled by boundary conditions set by the sample size and shape, phonon confinement, and surface roughness. Thus, we can no more speak about a constant boundary relaxation time. Many studies have been made to explain the behavior of phonons at the boundary of the nanostructure. Some suggested specular transmission while others considered diffuse scattering [14]. In our model, we have derived expression for boundary scattering relaxation time for a cylindrical nanowire with a circular cross-section that governs specular and diffusive transmission in which the probability of each is determined by incident phonon frequency and velocity and surface irregularity.

The main purpose behind this thesis is to develop a predictive model for the lattice thermal conductivity in cylindrical and pristine nanowires. A derived formalism for the lattice thermal conductivity in infinite crystals is modified to apply to low dimensional materials taking into account the effect of size, boundaries and surface properties on the variation of the lattice thermal conductivity. We apply this model to calculate the thermal conductivity of silicon, germanium, and silicon-germanium alloys.

The thesis is organized as follows. The second chapter governs a literature review of the work done in the field of the lattice thermal conductivity in bulk crystals and nanowires including theories and experimental measurements.

The third chapter contains an overview of the phonon dispersion in bulk and the general formalism for the lattice thermal conductivity.

Chapter 4 and 5 present a detailed description of our model for pristine and cylindrical nanowires respectively. These chapters will include the details of calculating the Debye temperature and specific heat for each as a function of temperature to be employed later in the thermal conductivity expressions.

Chapter 6 is devoted to our obtained results with a comparison between calculations and reported experimental data.

Finally, Chapter 7 will display the conclusion and future work.

CHAPTER II

LITERATURE REVIEW

The demand for controlling heat transfer rate across materials for its fundamental technological application in electronic and energy conversion devices makes the modeling of thermal conductivity of several materials a critical issue. With the revolutionary advances in technology and industry, nanotechnology has enabled the design and fabrication of hybrid devices in which semiconductors are nanostructured and fused together in an intricate fashion to obtain superior device functionality [3]. In this regard, semiconductor nanoscale devices are at the heart of technology and serve as a platform for nanoscience and engineering. It is, therefore, important to understand theoretically and experimentally the physics behind the heat conduction from bulk semiconductors up to the nanoscale size. Generally, the thermal conductivity varies as a function of temperature and material, however, the surface characteristics, the sample size and the sample boundary in nano-materials give the thermal conductivity a geometry dependence. In what follows, we will provide a literature review of the different studies of the thermal conductivity at the macro and nanoscale including theoretical modeling and experiments.

A study of lattice thermal conductivity in which the heat is carried by the phonons is investigated through three approaches: relaxation time approximation, variational methods and Green function's approach. The first two considers a solution of the Boltzmann equation as a step to study lattice thermal conductivity, while the Green's function approach deals with the problem from a quantum statistics point of view. Studies and calculations to derive phonon relaxation times for different scattering

mechanisms were done by several researchers. Among them, we can mention the work of Casimir [15] who studied boundary scattering and proposed an equation, relating the boundary relaxation time to phonon velocity and sample size, known as Casimir limit. Klemens (1951) first provided the calculation of the phonon relaxation time due to phonon-point defect scattering where it is stronger than umklapp scattering [16]. Herring (1954) has calculated the contribution of low frequency longitudinal phonons to the thermal conductivity and obtained the expressions for phonon-phonon normal processes [17]. In his early work (1942), Pomeranchuk studied the effect of isotopes in phonon scattering and its impact on thermal conductivity [18]. Later on, Geballe and Hull [19] demonstrated the influence of isotopic composition on the maximum thermal conductivity and performed measurements on germanium samples.

Thermal conduction was also studied by Leibfried and Schlomann [20] who gave an expression for the phonon mean free path, controlled by the three phonon scattering, in terms of Debye frequency and Grüneisen parameter. The authors used variational methods to derive the thermal conductivity as a function of average atomic mass, average atomic volume, Debye temperature and Grüneisen parameter.

Callaway, in his model, presented a complete treatment of the problem as he derived an expression for the lattice thermal conductivity at low temperatures [9] in terms of adjustable parameters. The theory well fits experimental data at low temperatures. Later, several studies and modifications were presented by Holland, Asen-Palmer et al., and Morelli et al. The refined model provides a full theoretical description of the lattice thermal conductivity in bulk crystals and fits experimental data in wide temperature range.

Experimental techniques are in need for measuring the lattice thermal conductivity of solid materials. There are number of possible ways to measure the lattice thermal conductivity. At this point, we can list some basic ways of measurement. The steady-state technique performs measurement when the material under study is in equilibrium. The non-steady technique performs the measurement during the heat transfer process. The latter provides results quickly. The Comparative method is based on comparing thermal differences. In this technique, a sample of an unknown material is plugged between samples of known materials, where the heat flux through the unknown sample is to be calculated.

Another widely used method is the Guarded Hot Plate Method. A material sample is sandwiched between two plates. Temperature of the plates is recorded until it sets into a constant. The steady-state temperatures, sample thickness, and the hot plate heat input are employed to calculate thermal conductivity. Another method to mention is the Laser Flash Diffusivity used to measure the thermal diffusivity of different materials. An energy pulse (laser, flash lamp) heats the sample from one side and a detector on the other side detects the time-dependent temperature rise.

Till the moment, we have covered the main theories and models of the lattice thermal conductivity in bulk crystals and the accompanied experimental techniques. With the new developments in industry and the fabrication of nanostructured materials (nanowires, nanotubes, thin films, superlattices...), there is a growing interest in managing the thermal properties of such devices in the purpose of controlling its performance. Low dimensional materials show a clear reduction in the lattice thermal conductivity as the size of the sample, boundary conditions and surface asperities give the thermal conductivity a geometry dependence. In what follows, we will be interested

to discuss several studies carried out about the lattice thermal conductivity specifically in nanowires. Nanowires are materials that have different electrical, optical and thermal properties. Nanowires are candidates for photovoltaic devices, electrochemical energy storage, and thermoelectric applications. It has been found that low dimensional materials have higher thermoelectric property than their bulk counterparts what makes them extremely needed for power generation through thermoelectric conversion [21, 22]. We will report in the coming section various studies carried out to discuss the effect of size, boundary scattering, phonon confinement, isotopic composition and surface roughness on the lattice thermal conductivity of nanowires.

Ruf et al. [23] used a steady-state heat flow technique to measure the thermal conductivity in a bulk crystal of highly enriched silicon and natural silicon for temperatures between 2 and 310K. Thermal conductivity shows a maximum value of 30,000 $W.m^{-1}K^{-1}$ around 20K which is six times larger than that of natural silicon. Their results reveal that the maximum thermal conductivity k_m is strongly affected by the isotopic composition. This fact is then well described by Asen-Palmer and co-workers [11] who have measured the thermal conductivity of germanium crystals with different isotopic compositions. The work of Li et al. [24] on the thermal conductivity of individual silicon nanowires with different diameters followed. Using a microfabricated suspended device, the thermal conductivities of individual silicon nanowires with diameters of 22, 37, 56 and 115 nm were measured over a temperature range of 20-320K. The measurements showed a reduction of the lattice thermal conductivity up to two orders in comparison with the bulk value. The results show how the thermal conductivity in nanowires depends on the diameter, a factor that affects the phonon boundary scattering and phonon dispersion. Liang and Li [25] studied the size

dependence of thermal conductivity in nanoscale conducting systems. In their research, they presented a phenomenological theory for the size dependence of thermal conductivity and derived an analytical formula considering size confinement effects, surface scattering effects and mean free path. The model reveals that the size effect is dominant at the size about 5-100 nm and the surface scattering effect starts dominating at larger sizes. As the size reduces, the phonon-phonon interaction increases because of phonon confinement what decreases the thermal conductivity. The derived formula provides results that are in good agreement with experiments on Si and GaAs nanowires and thin films.

Mingo and other researchers [26] attempted to theoretically predict the thermal conductivity versus temperature dependence of Si and Ge nanowires. To do so, they tried first to use the traditional Callaway and Holland models to model the nanowire case, but those two approaches fail to provide physical reasonable results even for the qualitative behavior. The results from using Callaway and Holland's models for Silicon nanowires were shown as thermal conductivity versus temperature dependence curves for nanowires with different diameters. Their calculation using Callaway's model clearly doesn't agree with experimental results with a prediction error of 300% and more. With Holland's model, they got slightly better predictions, but still inaccurate. The two main factors leading to inappropriate predictions are: the use of modelistic phonon dispersion relations and the unsuitable anharmonic scattering relaxation times. As a correction, Mingo and co-workers employed real dispersion relations for the nanowires and predicted the thermal conductivity expression with no fitting parameters to any nanowire measurements. As for the result, an agreement is found between theoretical predictions and experimental sets for wider nanowires ranging between 37

and 115 nm wide. The prediction error was less than 15%. The narrowest of the wires (less than 30 nm) presents a curve that increases almost linearly from 50K up and its second derivative is positive between 50K and 320K. This implies that the wire contains vibrational modes with frequencies higher than the highest frequency available in bulk Si. The higher the frequency, the higher the inflection temperature is. These modes might be linked to the oxidation of the nanowire's surface, phonon confinement and nanowire low speed modes.

Huang and co-workers [27] attempted to develop an analytical form of the phonon boundary scattering rate in a semiconductor nanowire. The authors examined the effect of size confinement on phonon dispersion relations, phonon distribution and Debye temperature. The results reveal the decrease in the lattice thermal conductivity of nanowires as their diameters decrease. Other factors responsible for the drop in the thermal conductivity include boundary scattering effect, smaller phonon velocities, and reduced Debye temperature.

Hochbaum et al. [28] reported the decrease in the thermal conductivity of rough Si nanowires having Seebeck coefficient and electrical sensitivity values that are the same as doped bulk silicon but show a decrease in the thermal conductivity. The difference between the thermal conductivity experimental behavior in bulk silicon and nanowires, regarding their differences in size and surface properties, was not explained at that time. The results presented by the authors indicate that Si nanowires with smooth surface exhibit a boundary scattering which is far from completely diffusive, what shows that some phonon physical mechanisms were not taken into account.

The effect of isotopic composition, phonon confinement, and surface roughness on the lattice thermal conductivity of silicon bulk and nanowires was studied

14

by Kazan et al. [29]. In their research, the authors analyzed the thermal conductivity of bulk silicon and nanowires taking into account the physical nature of the acoustic and optical phonon mechanisms. They have used Callaway solution for Boltzmann equation and established a formalism for the thermal conductivity that takes into account the phonon incidence angles. A detailed treatment of the decay of optical phonons into acoustic ones is presented. The commonly used expression for phonon-boundary scattering is modified to include a phonon specularity factor that depends on phonon frequency, incidence angle and surface roughness. Namely, the investigated model accounts as an explanation to the previous unexplained results by Ruf et al. [23], Li et al. [24] and Hochbaum et al. [28].

Later on, Kazan and Volz [30] presented a general model for the calculation of the lattice thermal conductivity in granular crystals. The interplay between boundary scattering and phonon anharmonic scattering is considered and the effect of the surface phonons on the thermal conductivity is taken into account. Boltzmann equation including spatial dependence of the phonon distribution function is solved and expressions of the scattering of the phonons by the boundaries are developed. Vibrational Parameters such as Debye temperature and Grüneisen parameter are derived as a function of temperature and crystallographic direction by using a lattice dynamics approach. In addition, the model provides a physical definition of the widely used phonon specularity factor. The accuracy of the model has been demonstrated with reference to experimental measurements taking into account the surface direction effect and the effect of grain size and shape on the lattice thermal conductivity tensor in granular crystals.

CHAPTER III

PHONON DISPERSION IN BULK AND GENERAL FORMALISM OF THERMAL CONDUCTIVITY

In solids, heat energy is transmitted by phonons. In the presence of temperature gradient, phonons are responsible for the propagation of thermal energy in the crystal. In what follows, we will report on the phonon dispersion in bulk crystals and present the general formalism of the lattice thermal conductivity.

A. Phonon Dispersion in Bulk

In the classical picture within the harmonic approximation, the atoms in a solid crystal held together in the form of a lattice and considered as joined by springs. When one or more atoms is displaced from its equilibrium position, an elastic vibrational wave travels through the crystal lattice transporting thermal energy with it. The key to understand the problem of lattice dynamics in the harmonic approximation is to find the normal modes of a crystal. In other words, our goal is to calculate the functional relation between the phonon frequencies (energies) and their wave vectors. The latter is so called phonon dispersion. A single normal mode of vibration is expressed as a travelling wave of the form Aexp[i(q.r-ωt)], where q reveals the direction of wave propagation, ω is the frequency of the wave and A is the amplitude of vibration [30]. The energies of the elastic normal modes of a crystal are quantized:

$$E = \hbar\omega \ (n+\tfrac{1}{2}) \tag{1}$$

Thus, a phonon is a quantum of energy accompanied with vibrations. As a matter of fact, the idea of a phonon comes from the relative motion of the atoms not the motion of

their center of mass, that's why theoretically a phonon in a crystal does not carry momentum. In practice, a momentum ℏq is assigned to a phonon in the qth mode. A phonon is a quasi-particle.

1. Phonon Statistics

The average number of phonons in the $\mathbf{q}^{th}$ mode in thermal equilibrium at temperature T is given by the Bose-Einstein distribution function:

$$n_q = \frac{1}{exp^{\frac{\hbar\omega}{k_B T}} - 1} \tag{2}$$

where k_B is Boltzmann's constant. We can deduce from this expression that at absolute zero temperature, there are no phonons in a crystal. At low temperatures, ℏω >> k_B, the phonon distribution function reduces to $\sim exp^{\frac{-\hbar\omega}{k_B T}}$ i.e. a small probability for a phonon to occur. At high temperatures, $k_B T$ >> ℏω, the expression deviates to $\sim k_B T/\hbar\omega$ and the concentration of phonons increases linearly with temperature.

2. Lattice Dynamics of a Linear Chain

a. Monoatomic Linear Chain

Consider a monatomic linear chain of N atoms separated "a" apart. Periodic, cyclic, Born-von Karman boundary conditions are assumed, so that the chain is closed and the (N+1)th atom is the 1st atom. Only the contribution of the nearest-neighbor forces is taken into account.
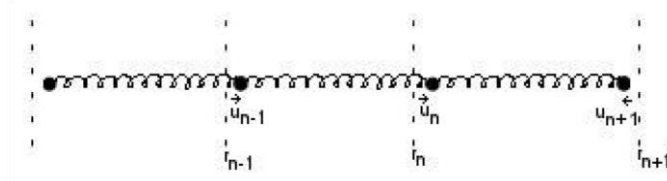
Figure 1: A monoatomic linear chain of N atoms separated "a" apart. [32]

Suppose that the nth atom in the chain has a displacement u_n from its equilibrium.
Applying Newton's second law and Hooke's law, the equation of motion of the nth atom
is:

$$m \frac{d^2 u_n}{dt^2} = \wedge \left[(u_{n+1} - u_n) + (u_{n-1} - u_n) \right] \tag{3}$$

where m is the mass of an atom and $\wedge$ is the nearest-neighbor force constant. We
attempt a solution of the form $u_n = A exp^{[i(qx - \omega t)]}.$ Note that we only have one
allowed mode of vibration here, either longitudinal or transverse. Replacing the
attempted solution in the equation of motion, we get:

$$\omega = 2 \sqrt{\frac{\wedge}{m}} \, | \sin(\mathbf{q}a/2) | \tag{4}$$

This is known as the phonon dispersion relation for the monatomic linear chain.

Figure 2: Phonon dispersion relation for the monoatomic linear chain. [33]

18

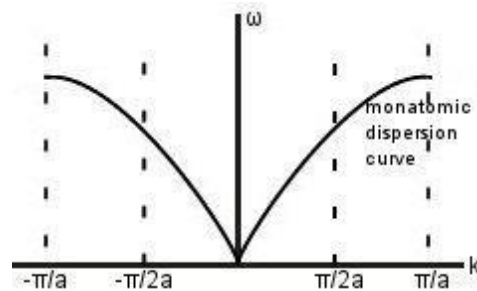The Brillouin zone is the line segment between $-\pi/a$ and π/a. It corresponds to the unit cell of a reciprocal lattice. The function ω (**q**) is a symmetric function between **q** and -**q**. It is trivial that there are N allowed values of **q** in the Brillouin zone of the linear chain. Therefore, there are N allowed normal modes of the linear chain.

In the long wavelength limit, $\mathbf{q} \to 0$, $\sin(\mathbf{q}a/2) \sim \mathbf{q}a/2$, and the phonon frequency reduces to: $\omega = a\sqrt{\dfrac{\wedge}{m}}\,\mathbf{q}$, thus $\omega^2 = \dfrac{\wedge}{a\,\rho}\,\mathbf{q}^2$. With the Young's modulus $E = \dfrac{\rho}{a}$, the dispersion relation converges to a linear one: $w = v_L \mathbf{q}$, where v_L is the longitudinal sound velocity.

b. Diatomic Linear Chain

      The problem of the lattice dynamics of crystals with a basis of more than one atom can be understood by studying the dynamics of a diatomic linear chain. Consider a long chain of 2N atoms forming N unit cells, each of length $2a$. Let m and M be the two masses of the basis. Similarly, Born-von Karman periodic boundary conditions is assumed and only neighbor forces are taken into account
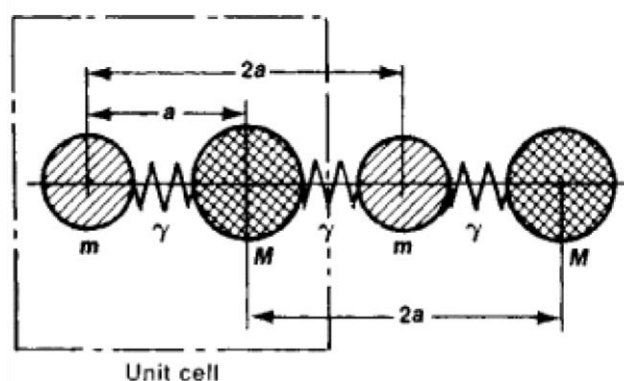
Figure 3: Diatomic linear chain. [34]

The equations of motion of each atom are:

$$m \left[\frac{d^2 u_{2n}}{dt^2}\right] = \gamma \left[u_{2n+1} + u_{2n-1} - 2u_n\right] \qquad (5)$$

and

$$M \left[\frac{d^2 u_{2n+1}}{dt^2}\right] = \gamma \left[u_{2n+2} + u_{2n} - 2u_{2n+1}\right] \qquad (6)$$

Trying solutions of the form: $u_{2n} = A_1 \, exp^{[i(2nqa - \omega t)]}$ and

$u_{2n+1} = A_2 exp^{[i(2n+1)qa - \omega t)]}$ and substituting them in the equations of motion, we get:

$$\omega^2 = \gamma \left(\frac{1}{m} + \frac{1}{M}\right) \pm \gamma \left[\left(\frac{1}{m} + \frac{1}{M}\right)^2 - \frac{4}{mM} \sin^2 qa\right]^{1/2} \qquad (7)$$
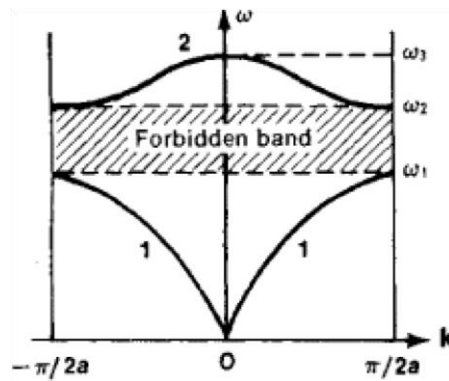
Figure:4 Phonon dispersion spectrum for a diatomic linear chain plotted in the 1st

Brillouin zone. [35]

(1) refers to the acoustic branch

(2) refers to the optical branch

with $\omega_1 = \left[\frac{2\gamma}{M}\right]^{1/2}$, $\omega_2 = \left[\frac{2\gamma}{m}\right]^{1/2}$, $\omega_3 = \left[2\gamma \left(\frac{1}{m} + \frac{1}{M}\right)\right]^{1/2}$.

The gap $(\omega_2 - \omega_1)$ in the spectrum is due to different atomic masses in the unit cell. The

number of allowed **q**-values is the number of unit cells that is 2N modes (2 accounts for

acoustic and optical).

20

3. Elastic Waves in Cubic Crystals

The equations of motion in a three-dimensional crystal in the long-wavelength limit can be expressed as:

$$\rho \ddot{u}_\alpha = \sum_{\alpha\beta\gamma\delta} C_{\alpha\beta\gamma\delta} \frac{\partial^2 \ddot{u}_\gamma}{\partial r_\delta \, \partial r_\beta} \tag{8}$$

where α, β, γ and δ are Cartesian coordinates, u_α is the displacement vector, $k_{(\gamma(\delta))}$ is the $\gamma(\delta)$ component of the wave vector, ρ is the mass density and $C_{\alpha\beta\gamma\delta}$ are the second-order elastic constants of the crystal. Using the trial function:

$$u = U \exp [i(\vec{\mathbf{q}}.\vec{r}) - \omega t] \tag{9}$$

and substituting it in the previous equation, we get:

$$\sum_{\delta\gamma} \sum_\beta C_{\alpha\beta\gamma\delta} q_\gamma q_\delta - \delta_{\alpha\beta} \, \rho\omega^2) u_\beta = 0 \tag{10}$$

where the first summation runs over β and the second one runs over $\delta\gamma$. These are known as the Green-Christoffel equations, whose solutions are obtained by solving the determinant:

$$| \sum C_{\alpha\beta\gamma\delta} \, \mathbf{q}_\gamma \mathbf{q}_\delta - \delta_{\alpha\beta} \, \rho\omega^2 | = 0 \tag{11}$$

The elastic tensor $C_{\alpha\beta\gamma\delta}$ is symmetric under the transpositions $\alpha\rightarrow\beta$, $\gamma\rightarrow\delta$, and $\alpha\beta \leftrightarrow \gamma\delta$. A simplified notation implies $11\rightarrow1$, $22\rightarrow2$, $33\rightarrow3$, 23, $32\rightarrow4$, 13, $31\rightarrow5$, 12, $21\rightarrow6$. The elastic constants of cubic crystals hold: $c_{11} = c_{22} = c_{33}$, $c_{12} = c_{13} = c_{23} = c_{31} = c_{32}$, $c_{44} = c_{55} = c_{66}$ and the others are zero.

On an attempt to find the longitudinal and transverse sound velocities, we consider waves where $\mathbf{q}$ is parallel to [100], [101], and [101]. Generally, $v=\sqrt{\dfrac{c_{eff}}{\rho}}$, where c_{eff} is an effective elastic constant, which is given for cubic crystals in the following table:

Mode	$\mathbf{q} \parallel$ [100]	$\mathbf{q} \parallel$ [101]	$\mathbf{q} \parallel$ [111]
L	C_{11}	$\frac{1}{2}(C_{11}+C_{12}+C_{44})$	$1/3(C_{11}+2C_{12}+4C_{44})$
T_1	C_{44}	C_{44}	$1/3 (C_{11}-C_{12}+C_{44})$
T_2	C_{44}	$\frac{1}{2}(C_{11}-C_{12})$	$1/3 (C_{11}-C_{12}+C_{44})$

Table 1. Elastic constants for cubic crystals for each branch along high symmetry directions.

From what we have demonstrated, we can note that an elastic wave is considered two waves propagated independently. One is called the longitudinal wave, where the displacement (u_x) is in the direction of propagation and is propagated with a velocity c_l. In the other transverse wave, the displacement u_y and u_z is in a plane perpendicular to the direction of propagation and is propagated with velocity c_t. The velocity of longitudinal waves is always greater than that of transverse waves. In an isotropic infinite crystal, elastic waves propagate along three different branches: 1 longitudinal and 2 transverse.

B. General Formalism of the Lattice Thermal Conductivity

The lattice thermal conductivity $\kappa(T)$ is defined as the ratio of the phonon heat current density to the temperature gradient. It can be shown to be

$$\kappa(T) = V_B \sum_j \sum_k \hbar\omega_j(k)\tilde{N}_j(k)\frac{\mathbf{v}_j(k)}{\nabla \mathbf{T}} \tag{12}$$

where the summation runs over all phonon wave vectors k and polarizations j. $\omega_j(k)$ and $\mathbf{v}_j(k)$ are the frequency and group velocity corresponding to wave vector k and polarization j, V_B is the volume of the Brillouin zone, and $\tilde{N}_j(k)$ is the deviation of the phonon distribution from equilibrium in the state k. $\tilde{N}_j(k)$ is defined as the difference between the phonon distribution out of equilibrium $N_j(k)$ and the Planck phonon distribution at equilibrium $\overline{N}_j(k)$. In order to evaluate $\kappa(T)$, it is more convenient to deal with the frequency distribution function, or frequency spectrum $g(\omega)$, than with the individual phonon modes frequencies $\omega_j(k)$. The total frequency distribution function is defined as

$$g(\omega) = \left(\frac{2\omega}{3rN_c}\right)\sum_j \sum_k \delta\left(\omega^2 - \omega_j^2(k)\right) \tag{13}$$

where r is the number of atoms per unit-cell, N_c is the number of unit-cells in the crystal and δ is the Dirac-Delta Function. It follows that the frequency distribution function of the jth phonon branch can be expressed as

$$g_j(\omega) = \left(\frac{2\omega}{3r(2\pi)^3}\right)V_B^{-1}\int \delta\left(\omega^2 - \omega_j^2(\mathbf{k})\right)d^3k \tag{14}$$

where the integral is carried out through the first Brillouin zone. Now, if we change to spherical polar coordinates (k, θ, φ), and use the relation

$$\delta(f(x)) = \sum_i \frac{\delta(x - x_i)}{|f'(x_i)|} \tag{15}$$

where $\{x_i\}$ are simple zeros of $f(x)$, Eq.14 is transformed into

$$g_j(\omega) = \frac{1}{3r(2\pi)^3 V_B} \int_0^\pi \sin \theta d\theta \int_0^{2\pi} d\varphi k_j^2(\omega, \theta, \varphi) \frac{dk_j(\omega, \theta, \varphi)}{d\omega} \tag{16}$$

where $k_j(\omega, \theta, \varphi)$ is the solution to $\omega = \omega_j(k, \theta, \varphi)$. This means that the quantity

$\frac{1}{3r(2\pi)^3 V_B} k_j^2(\omega, \theta, \varphi) dk_j(\omega, \theta, \varphi)$ is the frequency distribution function per unit solid

angle for the *jth* branch of the total phonon spectrum. Let us denote this quantity by

$g_j(\omega, \theta, \varphi)$. Expressing the phonon spectrum of the jth branch $g_j(\omega)$ in the form of

Eq.(16) allows evaluating $g_j(\omega)$ by using Houston's method. The idea behind Houston's

method is briefly as follows. The function $g_j(\omega, \theta, \varphi)$ has a cubic symmetry in θ and φ

because the normal mode frequencies are invariant with respect to any real orthogonal

transformation of axes which takes the crystal to itself. This means that $g_j(\omega, \theta, \varphi)$ can

be expanded in terms of Kubic harmonics, K_m which have the symmetry of the lattice,

$$g_j(\omega, \theta, \varphi) = \sum_{m=0}^{\infty} {}'a_m(\omega) K_m(\theta, \varphi) \tag{17}$$

where $K_0 = 1$ and the prime on the summation means that the term corresponding to

$m = 1$ is omitted from the summation. The K_m satisfy the orthogonality condition

$$\int_0^\pi \sin\theta d\theta \int_0^{2\pi} d\varphi K_m(\theta,\varphi)K_n(\theta,\varphi) = 4\pi\gamma_m\delta_{mn} , \qquad (18a)$$

where γ_m is a normalization constant and δ_{mn} is the usual Kronecker symbol. The method

for generating γ_m and the Kubic harmonics are reported. The first few γ_m are

$$\gamma_0 = 1,$$
$$\gamma_1 = 0,$$
$$\gamma_2 = {16}/{3.5.5.7},$$
$$\gamma_3 = {32}/{(3.7.11)^2.13}, \qquad (18b)$$
$$\gamma_4 = {256}/{(33.(65)^2.17)},$$
$$\gamma_5 = {2560}/{(91.(11.17.19)^2)},$$
$$\gamma_6 = {41984}/{(11.(13.17.19.21.23)^2)},$$

and the first six Kubic harmonics are

$$K_0 = 1,$$
$$K_1 = 0,$$
$$K_2 = x^4 + y^4 + z^4 - {3}/{5}\rho^4,$$
$$K_3 = x^2 y^2 z^2 + {1}/{22}\rho^2 K_2,$$
$$K_4 = x^8 + y^8 + z^8 - {28}/{5}\rho^2 K_3 - {210}/{143}\rho^4 K_2 - {1}/{3}\rho^8,$$
$$K_5 = x^{10} + y^{10} + z^{10} - {45}/{19}\rho^2 K_4 - {126}/{17}\rho^4 K_3 - {210}/{143}\rho^6 K_2 - {3}/{11}\rho^{10},$$
$$K_6 = x^4 y^4 z^4 + {6}/{115}\rho^2 K_5 - {1}/{266}\rho^4 K_4 - {54}/{1615}\rho^6 K_3 + {3}/{2431}\rho^8 K_2 - {1}/{5005}\rho^{12},$$

(18c)

where $\rho^2 = x^2 + y^2 + z^2$. Now, if we substitute Eq.(17) into Eq.(16) and make use of

Eq.(18a), we obtain

$$g_j(\omega) = 4\pi a_0(\omega). \qquad (19)$$

The coefficient $a_0(\omega)$ can be obtained by following Houston's procedures. It can be considered that there exist directions in Fourier space along which the cubic crystal dynamical matrix factors into equations of low degree in ω^2 which can be solved exactly for ω as a function of the wave vector k. These directions are high symmetry directions such as (100), (110), and (111) directions. Along these directions, the equation $\omega = \omega_j(k, \theta, \varphi)$ can be expressed as $\omega = \omega_j(k_s, \theta_s, \varphi_s)$. Since these equations can be inverted exactly to obtain k for simple enough models, it follows that $g_j(\omega, \theta_s, \varphi_s)$ can be exactly obtained for these special directions. If we then retain as many terms in Eq.17 as the number of directions (θ_s, φ_s), the $a_m(\omega)$ in Eq.17 are given as the solution of a set of simultaneous linear equations whose coefficients are the values of $g_j(\omega, \theta, \varphi)$ along the direction (θ_s, φ_s). In particular, it follows from Eq.17, Eq.18, and Eq.19 that the total frequency distribution function for the jth branch can be expressed in terms of the frequency distribution functions along the (100), (110), (111), (210), (211), and (221) directions (which in principal can be obtained with satisfactory accuracy) as

$$g_{j,1}(\omega) = \frac{4\pi}{35}\left[10g_j^{(A)}(\omega) + 16g_j^{(B)}(\omega) + 9g_j^{(C)}(\omega)\right]$$

$$g_{j,2}(\omega) = \frac{4\pi}{945}\left[45g_j^{(A)}(\omega) + 32g_j^{(B)}(\omega) + 243g_j^{(C)}(\omega) + 625g_j^{(D)}(\omega)\right],$$

$$g_{j,3}(\omega) = \frac{4\pi}{35}\left[6g_j^{(A)}(\omega) + 8g_j^{(B)}(\omega) - 3g_j^{(C)}(\omega) + 24g_j^{(E)}(\omega)\right],$$

$$g_{j,4}(\omega) = \frac{4\pi}{70}\left[17g_j^{(A)}(\omega) - 64g_j^{(B)}(\omega) - 125g_j^{(C)}(\omega) + 243g_j^{(F)}(\omega)\right],$$

$$g_{j,5}(\omega) = \frac{4\pi}{10395}\left[\begin{array}{l}1197g_j^{(A)}(\omega) + 1456g_j^{(B)}(\omega) + 729g_j^{(C)}(\omega) + 3125g_j^{(D)}(\omega)\\ +3888g_j^{(E)}(\omega)\end{array}\right],$$

$$g_{j,6}(\omega) = \frac{4\pi}{83160}\left[\begin{array}{l}7281g_j^{(A)}(\omega) - 13312g_j^{(B)}(\omega) - 13608g_j^{(C)}(\omega) + 43750g_j^{(D)}(\omega)\\ +59049g_j^{(F)}(\omega)\end{array}\right],$$

$$g_{j,7}(\omega) = \frac{4\pi}{770}\left[\begin{array}{l}117g_j^{(A)}(\omega) + 416g_j^{(B)}(\omega) + 294g_j^{(C)}(\omega) + 672g_j^{(E)}(\omega)\\ -729g_j^{(F)}(\omega)\end{array}\right],$$

$$g_{j,8}(\omega) = \frac{4\pi}{1081080}\left[\begin{array}{l}117603g_j^{(A)}(\omega) + 76544g_j^{(B)}(\omega) + 17496g_j^{(C)}(\omega) + 381250g_j^{(D)}(\omega)\\ +311040g_j^{(E)}(\omega) + 177147g_j^{(F)}\end{array}\right],$$

(20)

Where the superscripts A, B, C, D, E, and F on g signify (100), (110), (111) (210), (211), and (221) respectively.

The evaluation of $g_j^{(A)}(\omega)$, $g_j^{(B)}(\omega)$, $g_j^{(C)}(\omega)$, $g_j^{(D)}(\omega)$, $g_j^{(E)}(\omega)$, and $g_j^{(F)}(\omega)$ can be simplified by noting that Houston's method illustrated above can be used for the approximate evaluation of any integral of the form

$$J = \int_0^\pi \sin\theta d\theta \int_0^{2\pi} d\varphi I(\theta,\varphi), \tag{21}$$

provided that $I(\theta,\varphi)$ has cubic symmetry. From the general form of a three-dimensional dynamical matrix one can find that the leading term in the expansion of $\omega_j^2(\mathbf{k})$ is of $O(k^2)$ For small values of k, which are the only excited wave vectors at low temperatures, we must have

$$\omega_j^2(\mathbf{k}) = C_j^2(\theta,\varphi)k^2 + D_j^2(\theta,\varphi)k^4 + ... , \tag{22}$$

where the coefficients C_j and D_j have the symmetry of the lattice. Upon inverting Eq. (22), we find the frequency distribution function per unit solid angle for the jth branch of the spectrum

$$g_j(\omega,\theta,\varphi) = \frac{1}{3rv_B} \frac{1}{(2\pi)^3} \left[\frac{\omega^2}{C_j^3(\theta,\varphi)} - \frac{5}{2} \frac{D_j^2(\theta,\varphi)}{C_j^7(\theta,\varphi)} \omega^4 + ... \right] \tag{23}$$

On the other hand, for small values of ω, the phonon spectrum of a three-dimensional crystal has the expansion

$$g(\omega) = a_2\omega^2 + a_4\omega^4 + ... \tag{24}$$

Thus, from Eq.(16), Eq.(23), and Eq.(24) we find that

$$a_2 = \frac{1}{3rv_B} \frac{1}{(2\pi)^3} \sum_j \int_0^\pi \int_0^{2\pi} \frac{\sin\theta d\theta d\varphi}{C_j^3(\theta,\varphi)} , \tag{25}$$

and

$$a_4 = -\frac{5}{2} \frac{1}{3rv_B} \frac{1}{(2\pi)^3} \sum_j \int_0^\pi \int_0^{2\pi} \frac{D_j^2(\theta,\varphi)\sin\theta d\theta d\varphi}{C_j^7(\theta,\varphi)} . \tag{26}$$

It is clear from Eq.(22) that the coefficients $C_j(\theta,\varphi)$ are the phonon group velocities for a given direction (θ,φ) of propagation. Thus, by applying Houston's method Eq.(21) to the evaluation of the integral in Eq.(25), we find that the coefficients of the low frequency end of the phonon spectrum can be expressed in terms of directional phonon group velocities as

$$a_2 = \frac{1}{3rV_B} \frac{1}{(2\pi)^3} 4\pi \sum_{[hkl]} \sum_j \frac{\chi_{[hkl]}}{v_{j,[hkl]}^3} , \tag{27}$$

Where $v_{j,[hkl]}$ the group velocity of the phonon of the jth is branch along the direction $[hkl]$ and $\chi_{[hkl]}$ is the weight of the contribution of the phonon spectrum in the direction $[hkl]$ to the total phonon spectrum according to Eq.(20). Hence, in view of Eq.(24), and assuming Debye-like dispersion relations, the phonon spectrum can be approximated by

$$g(\omega) = \frac{1}{3rV_B} \frac{1}{(2\pi)^3} 4\pi \sum_{[hkl]} \sum_{j} \frac{\chi_{[hkl]}}{v^3_{j,[hkl]}} \omega^2 \qquad (28)$$

The total phonon frequency distribution function $g(\omega)$ can thus be approximated as a weighted average of phonon spectra in high symmetry directions. In view of Eq.(12), Eq.(27), and Eq.(28), we can express the lattice thermal conductivity as

$$\kappa(T) = \frac{1}{3r(2\pi)^3} \sum_{[hkl]} \sum_{j} \frac{\chi_{[hkl]} \cos\psi_{[hkl]}}{v^2_{j,[hkl]}} \int_0^{\omega_{D,j,[hkl]}} \frac{\hbar\omega^3 . \tilde{N}_j(k)}{|\nabla \mathbf{T}|} d\omega \qquad (29)$$

Where the integrals upper limits $\omega_{D,j,[hkl]}$ are artificial limiting frequencies leading to correct normalization of $g_j^{([hkl])}(\omega)$, and ψ_{hkl} is the angle between the high-symmetry direction $[hkl]$ and the temperature gradient.

CHAPTER IV

THERMAL CONDUCTIVITY OF PRISTINE NANOWIRES

In this chapter, we aim to draw a theoretical understanding of the effects of the size and surface on the lattice thermal conductivity. So far, we have been dealing with infinite crystals having no borders and the Boltzmann equation is solved where the phonon distribution function has no spatial dependence. The geometry of the nanowires provides them a greater surface to volume ratio than their bulk counterparts. Thus, the behavior of phonons at the boundaries (surfaces, interfaces) plays an important role in their thermal transport properties. A better understanding of phonon dynamics at the boundaries is vital seeking a complete picture of the heat transport in nanowires. This different trend in the behavior of phonons in nanowires gives rise to the modification of acoustic phonon dispersion due to spatial confinement and change in the non-equilibrium phonon distribution function due to boundary scattering. As we will see, the phonon dispersion branches reveal a reduced average phonon group velocity. Heat transfer in pristine nanowires, nanowires with square cross-section, will be discussed in details in the following sections.

A. Vibrations and Deformations in Rods

Unlike bulk crystals, where phonons propagate along the longitudinal and transverse branches, phonons in a nanowire vibrate along three dispersion branches: longitudinal, torsional and bending.

1. Longitudinal Waves

A longitudinal deformation of the rod, with no external force on its sides, is a simple extension or compression propagated along its length. The wave equation is represented by:

$$\frac{\partial^2 u_z}{\partial z^2} - \frac{\rho}{E}\frac{\partial^2 u_z}{\partial t^2} = 0 \tag{30}$$

Seeking a solution of the form: $u_z = constant \times e^{[i\,(qz-\omega t)]}$

Upon substituting the solution in the wave equation, the velocity of propagation of longitudinal waves in nanowires is $\sqrt{\frac{E}{\rho}}$, where E is bulk Young's modulus and ρ is the bulk material's density, and

$$\omega = \sqrt{\frac{E}{\rho}}\,q \tag{31}$$

is the dispersion relation for the longitudinal branch. Comparing this velocity with the expression for $c_l = [\frac{E(1-\sigma)}{\rho(1+\sigma)(1-2\sigma)}]^{1/2}$, we find that it is less than the velocity of propagation of longitudinal waves in an infinite medium.

2. Bending Waves

A bent rod is stretched at some points and compressed at others. Lines on the convex side of the bent rod are extended and those on the concave side are compressed. There is a neutral surface between both that undergoes neither extension nor compression. Bending in rods induces bending (flexural) waves with small bending deflections. Equations of equilibrium for a slightly bent rod are:

$$\rho S\ddot{X} = EI_y \frac{\partial^4 X}{\partial z^4} \qquad \text{and} \qquad \rho S\ddot{Y} = EI_x \frac{\partial^4 Y}{\partial z^4} \tag{32}$$

Where ρS is the mass per unit length, and I_x and I_y are the moments of inertia with respect to x and y directions respectively.

We again seek a solution of the form:

$$X = \text{constant} \times e^{i\,(kz-\omega t)} \quad \text{and} \quad Y = \text{constant} \times e^{i\,(kz-\omega t)} \qquad (33)$$

Substituting the solutions above in the corresponding equations, we get the following dispersion relations

$$\omega = q^2 \left[\frac{EI_y}{\rho S}\right]^{1/2} \quad \text{and} \quad \omega = q^2 \left[\frac{EI_x}{\rho S}\right]^{1/2} \qquad (34)$$

For vibrations in the *x* and *y* directions respectively. The velocities of propagation are

$$V_x = 2q \left[\frac{EI_y}{\rho S}\right]^{1/2} \quad \text{and} \quad V_y = 2q \left[\frac{EI_x}{\rho S}\right]^{1/2} \qquad (35)$$

The bending wave speed is dispersive as it is proportional to the square root of frequency. Thus, higher frequency bending waves will travel faster than lower frequency ones. Flexural waves with different frequencies propagate with different speeds.

3. Torsional Waves

A torsional deformation is one in which each transverse section is rotated through some angle with respect to another one. The corresponding equation of motion is:

$$C \frac{\partial^2 \phi}{\partial^2 z} = \rho I \frac{\partial^2 \phi}{\partial^2 t} \qquad (36)$$

Where C is the torsional rigidity of the rod, ϕ being the angle of rotation of the cross-section, and I is the moment of inertia of the cross-section about its center of mass. With the same approach, we can see that the velocity of propagation of torsional vibrations along the nanowire is

$$\left[\frac{C}{\rho I}\right]^{\frac{1}{2}} \tag{37}$$

As we can see, acoustic phonon dispersion is modified in the case of nanowires.

Longitudinal and transverse branches in bulk crystals are replaced by longitudinal,

bending and torsional branches in nanowires. Note here that the surface phonons do not

contribute to the phonon averaged group velocity and just the volume phonons that

scatter by the surface do.

B. Allowable Normal Modes

Let us assume a rod of a square cross-section with dimensions $L_1 \times L_2 \times L_3$. Let

$U = (u, v, w)$ be the components of the displacement of a point in the solid. The

equations of motion of the solid are known as

$$\rho \frac{\partial^2 U}{\partial t^2} = \mu \, \nabla^2 U + (\lambda + \mu) \, \vec{\nabla} \, (\vec{\nabla}.U) \tag{38}$$

Where ρ is the density of the solid, μ and λ are Lame constants. For the boundary

conditions, we will assume that

$$u = 0 \qquad \frac{\partial v}{\partial x} = \frac{\partial w}{\partial x} = 0 \qquad x = 0, L_1 \tag{39}$$

$$v = 0 \qquad \frac{\partial u}{\partial y} = \frac{\partial w}{\partial y} = 0 \qquad y = 0, L_2 \tag{40}$$

$$w = 0 \qquad \frac{\partial u}{\partial z} = \frac{\partial v}{\partial z} = 0 \qquad z = 0, L_3 \tag{41}$$

These boundary conditions are particularly convenient for obtaining a simple solution to

equation (38). They show that the shear stresses are zero on the boundary of the rod and

that the motion perpendicular to the boundary is zero. Plugging in the boundary

conditions, the displacement of a point in a solid is:

$$U(x, y, z, t) = \sin\left(\frac{n_1 \pi x}{L_1}\right) \sin\left(\frac{n_2 \pi y}{L_2}\right) \sin\left(\frac{n_3 \pi z}{L_3}\right) e^{-i\omega t} \tag{42}$$

33

With substituting this solution in the equation of motion, we obtain the basic equation

for determining the normal mode frequencies:

$$[\frac{\rho\omega^2}{\pi^2} - (\lambda + 2\mu) \ [(\frac{n_1}{L_1})^2 + (\frac{n_2}{L_2})^2 + (\frac{n_3}{L_3})^2]] \ [\frac{\rho\omega^2}{\pi^2} - \mu \ [(\frac{n_1}{L_1})^2 + (\frac{n_2}{L_2})^2 + (\frac{n_3}{L_3})^2]] = 0 \qquad (43)$$

The solutions of this equation are:

$$\omega_L{}^2 = \frac{E}{\rho} \pi^2 \ [(\frac{n_1}{L_1})^2 + (\frac{n_2}{L_2})^2 + (\frac{n_3}{L_3})^2] \qquad (44)$$

$$\omega_B{}^2 = \frac{EI_{x,y}}{\rho S} \pi^4 \ [(\frac{n_1}{L_1})^2 + (\frac{n_2}{L_2})^2 + (\frac{n_3}{L_3})^2]^2 \qquad (45)$$

$$\omega_T{}^2 = \frac{C}{\rho I} \pi^2 \ [(\frac{n_1}{L_1})^2 + (\frac{n_2}{L_2})^2 + (\frac{n_3}{L_3})^2] \qquad (46)$$

C. Phonon Distribution Function and Boundary Scattering Rate

A pristine nanowire with a temperature gradient aligned parallel to the rod axis

in the *z* direction. In such a geometry, the thermal gradient pumps the phonons in the *z*

direction to every point of the cross-section of the nanowire at a rate independent of the

location in the cross-section. In the volume of the nanowire, these phonons lose their

momenta due to the resistive processes, while at a point close to the boundary of the rod

phonons tend to be absorbed by the surface. The latter induces the dependence of the

phonon heat flux on the distance from the boundary. The presence of borders allow the

resistive processes to dominate the normal ones. So, the variation of the phonon

distribution function with respect to position must be well considered in the Boltzmann

equation.

Spatial-dependent Boltzmann equation describing the rate of change in the

steady state phonon distribution can be written as

$$-\boldsymbol{v}. \nabla N + \frac{\partial N}{\partial t} = 0 \qquad (47)$$

34

The first and second terms describe the change in the phonon distribution due the presence of a temperature gradient and collision processes, respectively. It is customary to write the second term within the relaxation time approximation as $\frac{N_u - N}{\tau_N} + \frac{\overline{N} - N}{\tau_{U+I}}$ to account for the difference between the physical nature of the phonon normal processes, which tend to displace the Planck distribution, and that of the resistive processes, which tend to restore the phonon distribution back to its equilibrium value. Here, is the distribution at "flowing equilibrium" (or a displaced Planck distribution by a vector having the dimension of energy times length) and the characteristic times τ_N and τ_{U+I} are relaxation times associated with the phonon normal processes and resistive processes, respectively. The relaxation time associated with the resistive processes τ_{U+I} is defined as $\frac{1}{\tau_{U+I}} = \frac{1}{\tau_U} + \frac{1}{\tau_I}$, where τ_U and τ_I are relaxation times associated with Umklapp processes and phonon scattering by localized mass-difference, respectively. Klemen's theory can be used to calculate τ_I, and the conventional Fermi's golden rule formula based on the cubic harmonic part of the crystal Hamiltonian as perturbation can be used to calculate τ_N and τ_U. The Boltzmann equation takes the form

$$v_z \frac{dN}{dT} \frac{\partial T}{\partial z} + v_x \frac{\partial N}{\partial x} + v_y \frac{\partial N}{\partial y} + N\tau = 0 \tag{48}$$

It can be seen that the phonon distribution function has an explicit *x* and *y* dependence, with an implicit dependence on *z* through the temperature gradient. We can note here that in the very vicinity of the sample edge, parallel to the heat current, phonons are either at thermal equilibrium with the boundary or out of equilibrium due to interaction with surface phonons. At the opposite edge, phonons are either absorbed then reemitted back or reflected with opposite momentum and equilibrium phonon distribution. With these considerations, the solution takes the form [30]

$$N = \frac{P\tau}{2}[(1\text{-}\exp{(\frac{-x(y)}{\tau\,v_x}))} + (1\text{-}\exp{(\frac{-y(x)}{\tau\,v_y}))}] + \sigma_z \exp{(\frac{-x(y)}{\tau\,v_x})} + \sigma_z \exp{(\frac{-y(x)}{\tau\,v_y})}] \quad (49)$$

Where $P = v_z \frac{dN}{dt} \frac{\partial T}{\partial z}$ is the negative of the rate at which phonons are delivered to a unit

volume of the reciprocal space, x(y) is the y-dependent distance from the border parallel

to the x-axis, y(x) is the x-dependent distance from the border parallel to the y-axis, and

σ_z is the deviation of the phonon distribution due to interactions between volume

phonons and surface phonons [29]. Upon substituting equation (49) in (48), we find

$$P = (\frac{1}{\tau_{B,x}} + \frac{1}{\tau_{B,y}} + \frac{1}{\tau}) <\widetilde{N}> \quad (50)$$

With

$$\frac{1}{\tau_{B,\alpha}} = \frac{\iint v_\alpha \frac{\partial \widetilde{N}}{\partial \alpha} dx\, dy}{\iint \widetilde{N} dx\, dy} \quad (51)$$

Where $\alpha = x$ or y, and

$$<\widetilde{N}> = \frac{\iint \widetilde{N}\, dx\, dy}{\iint dx\, dy} \quad (52)$$

By using the equations above, the boundary scattering rates are given by [30]

$$\frac{1}{\tau_{B,x}} = \frac{v_x}{l_x} \frac{\left(1-\frac{2\sigma_z}{\tau P}\right)(1-exp(\frac{-l_x}{\tau v_x}))}{2-[\sum_\alpha \frac{\tau v_\alpha}{l_\alpha}(1-exp(\frac{-l_\alpha}{\tau v_\alpha})\left(1-\frac{2\sigma_z}{\tau P}\right)]} \quad (53)$$

$$\frac{1}{\tau_{B,y}} = \frac{v_y}{l_y} \frac{\left(1-\frac{2\sigma_z}{\tau P}\right)(1-exp(\frac{-l_y}{\tau v_y}))}{2-[\sum_\alpha \frac{\tau v_\alpha}{l_\alpha}(1-exp(\frac{-l_\alpha}{\tau v_\alpha})\left(1-\frac{2\sigma_z}{\tau P}\right)]} \quad (54)$$

Where l_x and l_y label the dimensions along the x-axis and y-axis, respectively. Note

here that τ is the relaxation time associated to resistive processes and that the borders

add resistance to the heat flux. In the case of completely diffusive boundaries, σ_z is

equal to zero. While, in the case of total specular phonon reflection, $\frac{P\tau}{2}$ must be remain

equal to σ_z to ensure that N reduces to τP at any position in the rod. However, in the

case of partial specular phonon reflection, the ratio of σ to τP must be equal to a positive

constant smaller than one so that N reduces fast to τP as the phonons move away from the boundaries of the nanowire. Thus, the term $\frac{2\sigma}{P\tau}$ employed in the phonon boundary scattering rates is always independent of the position in the crystal and has a magnitude between zero and one. Roughness plays an important role in phonon dynamics at the surface. Surface irregularities reduce the lifetime of a surface phonon and consequently reduce σ. Therefore, the term $\frac{2\sigma}{P\tau}$ has all the characteristics of the phonon specularity factor. The phonon specularity factor, which was originally derived by Ziman, depends on the characteristics of the incident phonon and surface asperities according to

$$p = \exp(-16\pi^2\lambda^2\omega^2/v^2) \tag{55}$$

Where λ is the root mean square (rms) surface irregularity. [30]

D. Relaxation Times for Various Phonon Processes

In this section, we will consider three scattering mechanisms:

-normal three phonon processes

-umklapp processes

-isotope scattering

The normal processes conserve the crystal momentum, while the other two are resistive processes.

1. Normal Three Phonon Processes

The energy of the crystal is described by a Hamiltonian *H*. The Hamiltonian *H* in the harmonic approximation is:

$$H = \frac{1}{2}\sum_m M\dot{u}_m^2 + \frac{1}{2}\sum_{m,n,i,j} A_{mn}^{ij}\, u_m^i u_n^j \tag{56}$$

The eigenstates corresponding to *H* are non-interacting phonons. In order to account for the interaction between phonons, namely the creation of a new phonon because of the decay of higher energy ones, and the annihilation of two low energy phonons to give a higher energy one, a higher order term $H^{(3)}(\mathbf{q})$:

$$H^{(3)}(\mathbf{q}) = \sum_{q,j,q',j',q'',j''} V_{(3)}(\mathbf{q}, j, \mathbf{q'}, j', \mathbf{q''}, j'') \, a \, (\mathbf{q}, j) \, a \, (\mathbf{q'}, j') \, a^+ \, (\mathbf{q''}, j'') \quad (57)$$

Where a and a^+ are creation and annihilation operators in which they operate on the harmonic oscillator coordinates. In the Hamiltonian above $H^{(3)}(\mathbf{q})$, we consider a normal process in which two phonons with wave vectors **q** and **q'** and polarizations j and j' merge into a higher energy phonon of wave vector **q''** and polarization j'', such that **q''**= **q** + **q'**. In this process, energy and crystal momentum are conserved. The appropriate expression for the relaxation time for longitudinal phonons was found to be [12]:

$$\tau_{N,L}^{-1} = B_{N,L} \omega^2 T^3 \tag{58}$$

And that for transversal phonons:

$$\tau_{N,T}^{-1} = B_{N,T} \omega T^4 \tag{59}$$

The coefficients $B_{N,L}$ and $B_{N,T}$ depend on the phonon velocity as the following:

$$B_{N,L} = \frac{k_B^3 \gamma_T^2 V}{M h^2 v_L^5} \quad \text{and} \quad B_{N,T} = \frac{k_B^4 \gamma_T^2 V}{M h^3 v_T^5} \tag{60}$$

Where γ_L and γ_T are the longitudinal and transversal Grüneisen constants.

2. Umklapp Three Phonon Processes

Umklapp process is a resistive process in which its presence induces a decay in the lattice thermal conductivity at high temperatures. In this process, the crystal momentum is not conserved, however the energy is. The vector sum of the initial phonon wave vectors is equal to the wave vector of the created phonon plus a reciprocal

lattice vector **G**. This process is described by the same anharmonic Hamiltonian term as the normal processes. It has been found that the corresponding scattering rate for phonons is given by [12]:

$$\tau_{U,L}^{-1} = B_{U,L}\omega^2 T \, exp \left(\frac{-\theta_{D,L}}{3T} \right) \tag{61}$$

for longitudinal process, and

$$\tau_{U,T}^{-1} = B_{U,T}\omega^2 T \, exp \left(\frac{-\theta_{D,T}}{3T} \right) \tag{62}$$

where the constants $B_{U,L}$ and $B_{U,T}$ are given by:

$$B_{U,L} = \frac{h\gamma_L^2}{M\theta_{D,L}v_L^2} \quad \text{and} \quad B_{U,T} = \frac{h\gamma_T^2}{M\theta_{D,T}v_T^2} \tag{63}$$

The above relaxation times corresponding to umklapp processes decay exponentially in the large temperature limit. It has been demonstrated to fit the thermal conductivity k(T) curves with acceptable phonon dispersion curve characteristics.

3. Isotope Scattering

Mass-difference or Point-Defect scattering is one of the phonon processes that influence the phonon lifetime, through which the random presence of isotopes in the host crystal changes the average mass and creates point defects. Klemens in his theory suggested an expression describing the rate at which phonons scatter by point-defects. For a given phonon branch j, the isotope scattering rate is given by [12]:

$$\tau_{I,j}^{-1} = \frac{V \, \Gamma}{4 \, \pi v_j^3} \, \omega^4 \tag{64}$$

Where V is the volume per atom and Γ is the mass-fluctuation-phonon scattering parameter given by:

$$\Gamma = \frac{\sum_i (c_i M_i)^2 - (\sum_i c_i M_i)^2}{(\sum_i c_i M_i)^2} \tag{65}$$

Where c_i and M_i correspond to the concentration and the mass of the constituent isotope respectively.

39

E. Phonon Density of States

Now we will derive the density of states g (ω), the fraction of normal modes with frequencies in the interval (ω, ω+dω). The number of longitudinal modes with frequencies less than ω is the number of positive integer lattice points (n_1, n_2, n_3) which obey:

$$\pi^2 v_L^2 \left[\left(\frac{n_1}{L_1}\right)^2 + \left(\frac{n_2}{L_2}\right)^2 + \left(\frac{n_3}{L_3}\right)^2 \right] \leq \omega^2 \tag{66}$$

That is, the number of lattice points lying within an octant of the ellipsoid specified by:

$$\frac{x^2}{L_1^2} + \frac{y^2}{L_2^2} + \frac{z^2}{L_3^2} = \frac{\omega^2}{\pi 2 \, v_L^2} \tag{67}$$

This number is equal to the area in the

$$\frac{\pi^2 v_L^2}{\omega^2 L_1^2} x^2 + \frac{\pi^2 v_L^2}{\omega^2 L_2^2} y^2 + \frac{\pi^2 v_L^2}{\omega^2 L_3^2} z^2 = 1 \tag{68}$$

Implies that
$$\frac{x^2}{\frac{\omega^2 L_1^2}{\pi^2 v_L^2}} + \frac{y^2}{\frac{\omega^2 L_2^2}{\pi^2 v_L^2}} + \frac{z^2}{\frac{\omega^2 L_3^2}{\pi^2 v_L^2}} = 1 \tag{69}$$

$$N_{\mathrm{L}}(\omega) = \frac{1}{8} \times \frac{4}{3} \pi \, a \, b \, c \qquad \text{where} \quad a = \frac{\omega L_1}{\pi v_L}, \, b = \frac{\omega L_2}{\pi v_L}, \, c = \frac{\omega L_3}{\pi v_L}$$

$$N_{\mathrm{L}}(\omega) = \frac{1}{6} \frac{L_1 L_2 L_3}{\pi^2} \frac{\omega^3}{v_L^3} \tag{70}$$

From its definition, the frequency spectrum or the density of states is given in terms of $N(\omega)$ by the relation:

$$g_{\mathrm{L}}(\omega) \, d\omega = \frac{1}{rN_c} \left[N(\omega + d\omega) - N(\omega) \right] = \frac{1}{rN_c} N'(\omega) \, d\omega$$

$$g_{\mathrm{L}}(\omega) \, d\omega = \frac{1}{2\pi^2} (L_1 L_2 L_3) \frac{1}{v_L^3} \omega^2 d\omega = \frac{V}{2\pi^2} \frac{1}{v_L^3} \omega^2 d\omega \tag{70a}$$

With a similar approach, we can find that the number of torsional modes of frequencies less than ω and is given by

$$N_T(\omega) = \frac{1}{6} \frac{L_1 L_2 L_3}{\pi^2} \frac{\omega^3}{v_T^3} \tag{71}$$

And $g_T(\omega)\, d\omega = \dfrac{V}{2\pi^2} \dfrac{1}{v_T^3}\, \omega^2 d\omega$ $\tag{71a}$

The number of bending modes with frequencies less than ω is the number of positive

integer lattice points (n_1, n_2, n_3) which obey:

$$\pi^2\, c_B\, [(\frac{n_1}{L_1})^2 + (\frac{n_2}{L_2})^2 + (\frac{n_3}{L_3})^2] \leq \omega \tag{72}$$

That is the number of lattice points lying within an octant of the ellipsoid specified by

$$\frac{x^2}{\frac{\omega L_1^2}{\pi^2 c_B}} + \frac{y^2}{\frac{\omega L_2^2}{\pi^2 c_B}} + \frac{z^2}{\frac{\omega L_3^2}{\pi^2 c_B}} = 1 \tag{73}$$

$$N_B(\omega) = \frac{1}{6} \frac{V}{\pi^2} \frac{\omega^{3/2}}{c_B^{3/2}} \tag{74}$$

And $g_B(\omega)\, d\omega = \dfrac{V}{4\pi^2} \dfrac{1}{c_B^{3/2}}\, \omega^{1/2} d\omega$ $\tag{74a}$

F. Formalism for the Lattice Thermal Conductivity in a Pristine Nanowire

The lattice thermal conductivity in the nanowire is given by

$$K = -\frac{1}{V} \sum_k \hbar\omega\, \widetilde{N}\, \frac{v_L}{\nabla T} \tag{75}$$

Where V is the volume of the first Brillouin zone, and thus

$$K = -\frac{1}{V} [\int_0^{\omega_{D,L}} \hbar\omega\, \widetilde{N}\, \frac{v_L}{\nabla T}\, g_L(\omega)d\omega + 4\int_0^{\omega_{D,T}} \hbar\omega\, \widetilde{N}\, \frac{v_L}{\nabla T}\, g_T(\omega)\, d\omega + 2\int_0^{\omega_{D,B}} \hbar\omega\, \widetilde{N}\, \frac{v_L}{\nabla T}\, g_B(\omega)\, d\omega \tag{76}$$

1. Derivation of the Deviated Phonon Distribution Function

In order to find $\widetilde{N}$, we follow Callaway's procedure. We know that the original

Boltzmann equation is:

$$v_z \frac{dN}{dt} \frac{\partial T}{\partial z} + v_x \frac{\partial N}{\partial x} + v_y \frac{\partial N}{\partial y} + N\tau = 0 \tag{77}$$

Moreover, it can be written as:

$$-v_L \frac{\partial N}{\partial z} + \frac{N_u - N}{\tau_N} + \frac{\bar{N} - N}{\tau_R} = 0 \qquad (78)$$

Where $\quad \frac{1}{\tau_R} = \frac{1}{\tau_U} + \frac{1}{\tau_I} + \frac{1}{\tau_B}\quad$, and since $N = \bar{N} + \tilde{N}$, we can write Boltzmann equation in

the form:

$$-v_L \frac{d\bar{N}}{dT} \frac{\partial T}{\partial z} + \frac{N_u - N}{\tau_N} - \frac{\tilde{N}}{\tau_R} = 0 \qquad (79)$$

On the other hand,

$$N_{\mathrm{u}} = \bar{N} + \frac{\vec{u}.\overrightarrow{k_z}}{k_B T} \frac{e^{\frac{\hbar\omega}{k_B T}}}{(e^{\frac{\hbar\omega}{k_B T}} - 1\ )^2} \qquad (80)$$

Where N_{u} is the displaced phonon distribution function due to normal processes and $\vec{u}$ is

a vector having the dimensions of energy x length describing the displacement of

Planck distribution and $\overrightarrow{k_z}$ is a wave vector in the z-direction i.e. the direction of

temperature gradient. Substituting equation (80) in (79), we get

$$-v_L \left[\frac{\hbar\omega}{k_B T^2} \frac{e^{\frac{\hbar\omega}{k_B T}}}{(e^{\frac{\hbar\omega}{k_B T}} - 1\ )^2}\right] \frac{\partial T}{\partial z} + \frac{1}{\tau_N}\left[\bar{N} + \frac{\vec{u}.\overrightarrow{k_z}}{k_B T} \frac{e^{\frac{\hbar\omega}{k_B T}}}{(e^{\frac{\hbar\omega}{k_B T}} - 1\ )^2} - N\right] - \frac{\tilde{N}}{\tau_R} = 0 \qquad (81)$$

Through some simplifications, Boltzmann equation reduces to

$$-v_L \left[\frac{\hbar\omega}{k_B T^2} \frac{e^{\frac{\hbar\omega}{k_B T}}}{(e^{\frac{\hbar\omega}{k_B T}} - 1\ )^2}\right] \frac{\partial T}{\partial z} + \frac{1}{\tau_N} \frac{\vec{u}.\overrightarrow{k_z}}{k_B T} \frac{e^{\frac{\hbar\omega}{k_B T}}}{(e^{\frac{\hbar\omega}{k_B T}} - 1\ )^2} - \left(\frac{1}{\tau_R} + \frac{1}{\tau_N}\right)\tilde{N} = 0 \qquad (82)$$

The combined relaxation time defined as:

$$\frac{1}{\tau_c} = \frac{1}{\tau_N} + \frac{1}{\tau_R} \qquad (83)$$

With
$$\tilde{N} = -\alpha\ v_L \frac{\partial T}{\partial z} \frac{\hbar\omega}{k_B T^2} \frac{e^{\frac{\hbar\omega}{k_B T}}}{(e^{\frac{\hbar\omega}{k_B T}} - 1\ )^2} \qquad (84)$$

Where α has the dimensions of a relaxation time. Substituting (84) and (83) in (82),

$$-v_L \frac{\hbar\omega}{k_B T^2} \frac{e^{\frac{\hbar\omega}{k_B T}}}{(e^{\frac{\hbar\omega}{k_B T}}-1)^2} \frac{\partial T}{\partial z} + \frac{1}{\tau_N} \frac{\vec{u}.\vec{k_z}}{k_B T} \frac{e^{\frac{\hbar\omega}{k_B T}}}{(e^{\frac{\hbar\omega}{k_B T}}-1)^2} - \frac{1}{\tau_c}\left[-\alpha\, v_L \frac{\partial T}{\partial z} \frac{\hbar\omega}{k_B T^2} \frac{e^{\frac{\hbar\omega}{k_B T}}}{(e^{\frac{\hbar\omega}{k_B T}}-1)^2}\right] = 0 \quad (85)$$

This equation simplifies to:

$$\frac{\vec{u}.\vec{k_z}}{\tau_N} + \frac{\alpha v_L}{\tau_c} \frac{\partial T}{\partial z} \frac{\hbar\omega}{T} = v_L \frac{\hbar\omega}{T} \frac{\partial T}{\partial z} \quad (86)$$

Since $\vec{u}$ is a constant vector in the direction of temperature gradient, we can express it as

$$\vec{u} = -\frac{\hbar}{T}\beta\, v_L^2 \frac{\partial T}{\partial z}\, \hat{z} \quad (87)$$

Where β has the dimension of a relaxation time and $k_z = \frac{\omega}{v_L}$.

Equation (86) can be written as:

$$\alpha = \tau_c \left(1 + \frac{\beta}{\tau_N}\right) \quad (88)$$

At this stage, we need to find β. That is why we make use of the fact that the normal processes conserve the crystal momentum. Thus, the rate of change of the total phonon momentum due to normal processes must be set equal to zero:

$$\sum_k \left(\frac{\partial N}{\partial t}\right)_N . \vec{K} = 0 \quad (89)$$

Implies that

$$\int_0^{\omega_D} \left(\frac{\partial N}{\partial t}\right)_N . \vec{K}\; g(\omega)d\omega = 0$$

$$= \int_0^{\omega_D} \frac{1}{\tau_{N,L}} \left[\bar{N} + \frac{1}{k_B T}\left(\frac{-\hbar\omega}{T}\beta v_L \frac{\partial T}{\partial z}\right) \frac{e^{\frac{\hbar\omega}{k_B T}}}{(e^{\frac{\hbar\omega}{k_B T}}-1)^2} - N\right].\vec{K}\; g_L(\omega)\; d\omega = 0$$

$$+ \int_0^{\omega_D} \frac{1}{\tau_{N,T}} \left[\bar{N} + \frac{1}{k_B T}\left(\frac{-\hbar\omega}{T}\beta v_L \frac{\partial T}{\partial z}\right) \frac{e^{\frac{\hbar\omega}{k_B T}}}{(e^{\frac{\hbar\omega}{k_B T}}-1)^2} - N\right].\vec{K}\; g_T(\omega)\; d\omega = 0 \quad (90)$$

$$+ \int_0^{\omega_D} \frac{1}{\tau_{N,B}} [\bar{N} + \frac{1}{k_B T} (\frac{-\hbar\omega}{T} \beta v_L \frac{\partial T}{\partial z}) \frac{e^{\frac{\hbar\omega}{k_B T}}}{(e^{\frac{\hbar\omega}{k_B T}}-1)^2} - N].\vec{K} \, g_B (\omega) \, d\omega = 0$$

Considering every branch separately, where $I_1 + I_2 + I_3 = 0$

$$I_1 = \int_0^{\omega_D} \frac{1}{\tau_{N,L}} [\bar{N} + \frac{1}{k_B T} (\frac{-\hbar\omega}{T} \beta v_L \frac{\partial T}{\partial z}) \frac{e^{\frac{\hbar\omega}{k_B T}}}{(e^{\frac{\hbar\omega}{k_B T}}-1)^2} - N].\vec{K} \, g_L (\omega) \, d\omega = 0$$

$$= \int_0^{\omega_D} \frac{e^{\frac{\hbar\omega}{k_B T}}}{(e^{\frac{\hbar\omega}{k_B T}}-1)^2} \frac{\hbar\omega}{k_B T^2} v_L \frac{\partial T}{\partial z} (\alpha - \beta) \frac{\vec{K}}{\tau_{N,L}} \, g_L (\omega) \, d\omega$$

$$= v_L \frac{\partial T}{\partial z} \int_0^{\omega_D} \frac{e^{\frac{\hbar\omega}{k_B T}}}{(e^{\frac{\hbar\omega}{k_B T}}-1)^2} \frac{\hbar\omega}{k_B T^2} (\tau_c (1 + \frac{\beta}{\tau_N}) - \beta) \frac{\vec{K}}{\tau_{N,L}} \, g_L (\omega) \, d\omega$$

$$= v_L \frac{\partial T}{\partial z} \int_0^{\omega_{D,L}} \frac{e^{\frac{\hbar\omega}{k_B T}}}{(e^{\frac{\hbar\omega}{k_B T}}-1)^2} \frac{\hbar\omega}{k_B T^2} (\tau_{c,L} + \beta (\frac{\tau_{c,L}}{\tau_{N,L}} - 1) \frac{\vec{K}}{\tau_{N,L}} \, g_L (\omega) \, d\omega \tag{91}$$

Similarly,

$$I_2 = v_L \frac{\partial T}{\partial z} \int_0^{\omega_{D,T}} \frac{e^{\frac{\hbar\omega}{k_B T}}}{(e^{\frac{\hbar\omega}{k_B T}}-1)^2} \frac{\hbar\omega}{k_B T^2} (\tau_{c,T} + \beta (\frac{\tau_{c,T}}{\tau_{N,T}} - 1) \frac{\vec{K}}{\tau_{N,T}} \, g_T (\omega) \, d\omega \tag{92}$$

$$I_3 = v_L \frac{\partial T}{\partial z} \int_0^{\omega_{D,B}} \frac{e^{\frac{\hbar\omega}{k_B T}}}{(e^{\frac{\hbar\omega}{k_B T}}-1)^2} \frac{\hbar\omega}{k_B T^2} (\tau_{c,B} + \beta (\frac{\tau_{c,B}}{\tau_{N,B}} - 1) \frac{\vec{K}}{\tau_{N,B}} \, g_B (\omega) \, d\omega \tag{93}$$

Having $I_1 + I_2 + I_3 = 0$ and substituting the wave vectors in terms of their dispersion relations:

$I_1 + I_2 + I_3$

$$= v_L \frac{\partial T}{\partial z} \int_0^{\omega_{D,L}} \frac{e^{\frac{\hbar\omega}{k_B T}}}{(e^{\frac{\hbar\omega}{k_B T}}-1)^2} \frac{\hbar\omega}{k_B T^2} (\tau_{c,L} + \beta (\frac{\tau_{c,L}}{\tau_{N,L}} - 1) \frac{\omega}{v_L} \frac{1}{\tau_{N,L}} \, g_L (\omega) \, d\omega$$

$$+ v_L \frac{\partial T}{\partial z} \int_0^{\omega_{D,T}} \frac{e^{\frac{\hbar\omega}{k_B T}}}{(e^{\frac{\hbar\omega}{k_B T}}-1)^2} \frac{\hbar\omega}{k_B T^2} (\tau_{c,T} + \beta (\frac{\tau_{c,T}}{\tau_{N,T}} - 1) \frac{\omega}{v_T} \frac{1}{\tau_{N,T}} \, g_T (\omega) \, d\omega$$

$$+ v_L \frac{\partial T}{\partial z} \int_0^{\omega_{D,B}} \frac{e^{\frac{\hbar\omega}{k_B T}}}{(e^{\frac{\hbar\omega}{k_B T}}-1)^2} \frac{\hbar\omega}{k_B T^2} \left(\tau_{c,B} + \beta \left(\frac{\tau_{c,B}}{\tau_{N,B}} - 1\right)\right) \frac{\omega^{1/2}}{c_B^{1/2}} \frac{1}{\tau_{N,B}} g_B(\omega) \, d\omega \tag{94}$$

$$= \int_0^{\omega_{D,L}} \frac{e^{\frac{\hbar\omega}{k_B T}}}{(e^{\frac{\hbar\omega}{k_B T}}-1)^2} \frac{\hbar\omega^4}{k_B T^2} \left[\frac{\tau_{c,L}}{\tau_{N,L}} + \beta \left(\frac{\tau_{c,L}-\tau_{N,L}}{\tau_{N,L}^2}\right)\right] \frac{1}{v_L^4} \, d\omega$$

$$+ \int_0^{\omega_{D,T}} \frac{e^{\frac{\hbar\omega}{k_B T}}}{(e^{\frac{\hbar\omega}{k_B T}}-1)^2} \frac{\hbar\omega^4}{k_B T^2} \left[\frac{\tau_{c,T}}{\tau_{N,T}} + \beta \left(\frac{\tau_{c,T}-\tau_{N,T}}{\tau_{N,T}^2}\right)\right] \frac{1}{v_T^4} \, d\omega$$

$$+ \int_0^{\omega_{D,B}} \frac{e^{\frac{\hbar\omega}{k_B T}}}{(e^{\frac{\hbar\omega}{k_B T}}-1)^2} \frac{\hbar\omega^2}{k_B T^2} \left(\frac{\tau_{c,B}}{\tau_{N,B}} + \beta \left(\frac{\tau_{c,B}-\tau_{N,B}}{\tau_{N,B}^2}\right)\right) \frac{1}{2c_B^2} \, d\omega \tag{95}$$

$$= \frac{1}{v_L^4} \frac{k_B^3 T^2}{\hbar^3} \int_0^{\omega_{D,L}} \frac{e^{\frac{\hbar\omega}{k_B T}}}{(e^{\frac{\hbar\omega}{k_B T}}-1)^2} \frac{\hbar^4\omega^4}{k_B^4 T^4} \left[\frac{\tau_{c,L}}{\tau_{N,L}} + \beta \left(\frac{\tau_{c,L}-\tau_{N,L}}{\tau_{N,L}^2}\right)\right] d\omega +$$

$$\frac{1}{v_T^4} \frac{k_B^3 T^2}{\hbar^3} \int_0^{\omega_{D,T}} \frac{e^{\frac{\hbar\omega}{k_B T}}}{(e^{\frac{\hbar\omega}{k_B T}}-1)^2} \frac{\hbar^4\omega^4}{k_B^4 T^4} \left[\frac{\tau_{c,T}}{\tau_{N,T}} + \beta \left(\frac{\tau_{c,T}-\tau_{N,T}}{\tau_{N,T}^2}\right)\right] d\omega +$$

$$\frac{1}{2c_B^2} \frac{k_B}{\hbar} \int_0^{\omega_{D,B}} \frac{e^{\frac{\hbar\omega}{k_B T}}}{(e^{\frac{\hbar\omega}{k_B T}}-1)^2} \frac{\hbar^2\omega^2}{k_B^2 T^2} \left[\frac{\tau_{c,B}}{\tau_{N,B}} + \beta \left(\frac{\tau_{c,B}-\tau_{N,B}}{\tau_{N,B}^2}\right)\right] d\omega \tag{96}$$

Introducing the dimensionless parameter $x = \frac{\hbar\omega}{k_B T}$,

$$= \frac{1}{v_L^4} \left(\frac{k_B T}{\hbar}\right)^2 \int_0^{\frac{\Theta_{D,L}}{T}} \frac{x^4 e^x}{(e^x-1)^2} \left[\frac{\tau_{c,L}}{\tau_{N,L}} + \beta \left(\frac{\tau_{c,L}-\tau_{N,L}}{\tau_{N,L}^2}\right)\right] dx +$$

$$\frac{1}{v_T^4} \left(\frac{k_B T}{\hbar}\right)^2 \int_0^{\frac{\Theta_{D,T}}{T}} \frac{x^4 e^x}{(e^x-1)^2} \left[\frac{\tau_{c,T}}{\tau_{N,T}} + \beta \left(\frac{\tau_{c,T}-\tau_{N,T}}{\tau_{N,T}^2}\right)\right] dx +$$

$$\frac{1}{2c_B^2} \int_0^{\frac{\Theta_{D,B}}{T}} \frac{x^2 e^x}{(e^x-1)^2} \left[\frac{\tau_{c,B}}{\tau_{N,B}} + \beta \left(\frac{\tau_{c,B}-\tau_{N,B}}{\tau_{N,B}^2}\right)\right] dx \tag{97}$$

$$= \frac{1}{v_L^4} \left(\frac{k_B T}{\hbar}\right)^2 \int_0^{\frac{\Theta_{D,L}}{T}} \frac{x^4 e^x}{(e^x-1)^2} \frac{\tau_{c,L}}{\tau_{N,L}} \, dx + \beta \frac{1}{v_L^4} \left(\frac{k_B T}{\hbar}\right)^2 \int_0^{\frac{\Theta_{D,L}}{T}} \frac{x^4 e^x}{(e^x-1)^2} \left(\frac{\tau_{c,L}-\tau_{N,L}}{\tau_{N,L}^2}\right) dx +$$

$$\frac{2}{v_T^4} \left(\frac{k_B T}{\hbar}\right)^2 \int_0^{\frac{\Theta_{D,T}}{T}} \frac{x^4 e^x}{(e^x-1)^2} \frac{\tau_{c,T}}{\tau_{N,T}} \, dx + \beta \frac{1}{v_T^4} \left(\frac{k_B T}{\hbar}\right)^2 \int_0^{\frac{\Theta_{D,T}}{T}} \frac{x^4 e^x}{(e^x-1)^2} \left(\frac{\tau_{c,T}-\tau_{N,T}}{\tau_{N,T}^2}\right) dx +$$

$$\frac{1}{2c_B^2} \int_0^{\frac{\Theta_{D,B}}{T}} \frac{x^2 e^x}{(e^x-1)^2} \frac{\tau_{c,B}}{\tau_{N,B}} \, dx + \beta \frac{1}{2c_B^2} \int_0^{\frac{\Theta_{D,B}}{T}} \frac{x^2 e^x}{(e^x-1)^2} \left(\frac{\tau_{c,B}-\tau_{N,B}}{\tau_{N,B}^2}\right) dx = 0 \tag{98}$$

So,

$\beta =$

$$\frac{\frac{1}{v_L^4}(\frac{k_B T}{\hbar})^2 \int_0^{\frac{\Theta_{D,L}}{T}} \frac{x^4 e^x}{(e^x-1\ )^2} \frac{\tau_{c,L}}{\tau_{N,L}} dx + \frac{2}{v_T^4}(\frac{k_B T}{\hbar})^2 \int_0^{\frac{\Theta_{D,T}}{T}} \frac{x^4 e^x}{(e^x-1\ )^2} \frac{\tau_{c,T}}{\tau_{N,T}} dx + \frac{1}{2c_B^2} \int_0^{\frac{\Theta_{D,B}}{T}} \frac{x^2 e^x}{(e^x-1\ )^2} \frac{\tau_{c,B}}{\tau_{N,B}} dx}{\frac{1}{v_L^4}(\frac{k_B T}{\hbar})^2 \int_0^{\frac{\Theta_{D,L}}{T}} \frac{x^4 e^x}{(e^x-1\ )^2}\left(\frac{\tau_{c,L}-\tau_{N,L}}{\tau_{N,L}^2}\right)dx + \frac{1}{v_T^4}(\frac{k_B T}{\hbar})^2 \int_0^{\frac{\Theta_{D,T}}{T}} \frac{x^4 e^x}{(e^x-1\ )^2}\left(\frac{\tau_{c,T}-\tau_{N,T}}{\tau_{N,T}^2}\right)dx + \frac{1}{2c_B^2}\int_0^{\frac{\Theta_{D,B}}{T}} \frac{x^2 e^x}{(e^x-1\ )^2}\left(\frac{\tau_{c,B}-\tau_{N,B}}{\tau_{N,B}^2}\right)}$$

(99)

Back to the thermal conductivity expression and plugging equations (70a), (71a), (74a), and (84) in (76), we get

$$K = \int_0^{\omega_{D,L}} \tau_{c,L}\left(1 + \frac{\beta}{\tau_{N,L}}\right) \frac{1}{v_L} \frac{1}{2\pi^2} \frac{\hbar^2 \omega^4}{k_B T^2} \frac{e^{\frac{\hbar\omega}{k_B T}}}{(e^{\frac{\hbar\omega}{k_B T}}-1\ )^2} d\omega +$$

$$4 \int_0^{\omega_{D,T}} \tau_{c,T}\left(1 + \frac{\beta}{\tau_{N,T}}\right) \frac{v_L^2}{v_T^3} \frac{1}{2\pi^2} \frac{\hbar^2 \omega^4}{k_B T^2} \frac{e^{\frac{\hbar\omega}{k_B T}}}{(e^{\frac{\hbar\omega}{k_B T}}-1\ )^2} d\omega +$$

$$2 \int_0^{\omega_{D,B}} \tau_{c,B}\left(1 + \frac{\beta}{\tau_{N,B}}\right) \frac{v_L^2}{c_B^{3/2}} \frac{1}{4\pi^2} \frac{\hbar^2 \omega^{5/2}}{k_B T^2} \frac{e^{\frac{\hbar\omega}{k_B T}}}{(e^{\frac{\hbar\omega}{k_B T}}-1\ )^2} d\omega$$

(100)

$$= \frac{1}{v_L} \frac{1}{2\pi^2} \frac{k_B^3 T^2}{\hbar^2} \int_0^{\omega_{D,L}} \tau_{c,L}\left(1 + \frac{\beta}{\tau_{N,L}}\right) \frac{\hbar^4 \omega^4}{k_B^4 T^2} \frac{e^{\frac{\hbar\omega}{k_B T}}}{(e^{\frac{\hbar\omega}{k_B T}}-1\ )^2} d\omega +$$

$$\frac{2v_L^2}{v_T^3} \frac{1}{\pi^2} \frac{k_B^3 T^2}{\hbar^2} \int_0^{\omega_{D,T}} \tau_{c,T}\left(1 + \frac{\beta}{\tau_{N,T}}\right) \frac{\hbar^4 \omega^4}{k_B^4 T^4} \frac{e^{\frac{\hbar\omega}{k_B T}}}{(e^{\frac{\hbar\omega}{k_B T}}-1\ )^2} d\omega +$$

$$+ \frac{v_L^2}{c_B^{3/2}} \frac{1}{2\pi^2} \frac{k_B^{3/2} T^{1/2}}{\hbar^{1/2}} \int_0^{\omega_{D,B}} \tau_{c,B}\left(1 + \frac{\beta}{\tau_{N,B}}\right) \frac{\hbar^{5/2} \omega^{5/2}}{k_B^{5/2} T^{5/2}} \frac{e^{\frac{\hbar\omega}{k_B T}}}{(e^{\frac{\hbar\omega}{k_B T}}-1\ )^2} d\omega$$

(101)

Introducing the dimensionless parameter $x = \frac{\hbar\omega}{k_B T}$,

$$K = \frac{1}{v_L} \frac{1}{2\pi^2} \frac{k_B^3 T^2}{\hbar^2} \frac{k_B T}{\hbar} \int_0^{\frac{\Theta_{D,L}}{T}} \tau_{c,L}\left(1 + \frac{\beta}{\tau_{N,L}}\right) \frac{x^4 e^x}{(e^x-1\ )^2} dx +$$

$$\frac{2v_L^2}{v_T^3} \frac{1}{\pi^2} \frac{k_B^3 T^2}{\hbar^2} \frac{k_B T}{\hbar} \int_0^{\frac{\Theta_{D,T}}{T}} \tau_{c,T}\left(1 + \frac{\beta}{\tau_{N,T}}\right) \frac{x^4 e^x}{(e^x-1\ )^2} dx +$$

$$\frac{v_L^2}{c_B^{3/2}} \frac{1}{2\pi^2} \frac{k_B^{3/2} T^{1/2}}{\hbar^{1/2}} \frac{k_B T}{\hbar} \int_0^{\frac{\Theta_{D,B}}{T}} \tau_{c,B}\left(1 + \frac{\beta}{\tau_{N,B}}\right) \frac{x^{5/2} e^x}{(e^x-1\ )^2} dx$$

(102)

46

$$K = \frac{1}{v_L} \frac{1}{2\pi^2} \frac{k_B^4 T^3}{\hbar^3} \left[I_{1,L} + \beta\, I_{2,L} \right] + \frac{2v_L^2}{v_T^3} \frac{1}{\pi^2} \frac{k_B^4 T^3}{\hbar^3} \left[I_{1,T} + \beta\, I_{2,T} \right] + \frac{v_L^2}{c_B^{3/2}} \frac{1}{2\pi^2} \frac{k_B^{5/2} T^{3/2}}{\hbar^{3/2}} [I_{1,B} + \beta I_{2,B}]$$

(103)

Where

$$I_{1,L} = \int_0^{\frac{\Theta_{D,L}}{T}} \tau_{c,L} \frac{x^4 e^x}{(e^x - 1\ )^2}\, dx$$

$$I_{2,L} = \int_0^{\frac{\Theta_{D,L}}{T}} \frac{\tau_{c,L}}{\tau_{N,L}} \frac{x^4 e^x}{(e^x - 1\ )^2}\, dx$$

$$I_{1,T} = \int_0^{\frac{\Theta_{D,T}}{T}} \tau_{c,T} \frac{x^4 e^x}{(e^x - 1\ )^2}\, dx$$

$$I_{2,T} = \int_0^{\frac{\Theta_{D,T}}{T}} \frac{\tau_{c,T}}{\tau_{N,T}} \frac{x^4 e^x}{(e^x - 1\ )^2}\, dx$$

$$I_{1,B} = \int_0^{\frac{\Theta_{D,B}}{T}} \tau_{c,B} \frac{x^{5/2} e^x}{(e^x - 1\ )^2}\, dx$$

$$I_{2,B} = \int_0^{\frac{\Theta_{D,B}}{T}} \frac{\tau_{c,B}}{\tau_{N,B}} \frac{x^{5/2} e^x}{(e^x - 1\ )^2}\, dx$$

(103a)

G. Derivation of the Crystal Vibrational Parameters

1. Specific Heat and Debye Temperature

The total energy associated with the nanowire normal modes can be written as

$$E = \sum_k \left(\frac{\hbar\omega}{2} + \frac{\hbar\omega}{e^{\frac{\hbar\omega}{k_B T}} - 1} \right)$$

(104)

The specific heat is given by:

$$C_v = \frac{\partial E}{\partial T}$$

$$= \sum_k \frac{\partial}{\partial T} \left(\frac{\hbar\omega}{e^{\frac{\hbar\omega}{k_B T}} - 1} \right)$$

$$= \sum_k \frac{\hbar^2 \omega^2}{k_B T^2} \frac{e^{\frac{\hbar\omega}{k_B T}}}{(e^{\frac{\hbar\omega}{k_B T}} - 1)^2}$$

$$= \int_0^{\omega_D} \frac{\hbar^2 \omega^2}{k_B T^2} \frac{e^{\frac{\hbar\omega}{k_B T}}}{(e^{\frac{\hbar\omega}{k_B T}} - 1)^2} \, g(\omega) \, d\omega \tag{104a}$$

The specific heat due to longitudinal phonons:

$$C_{v,L} = \int_0^{\omega_D} \frac{\hbar^2 \omega^2}{k_B T^2} \frac{e^{\frac{\hbar\omega}{k_B T}}}{(e^{\frac{\hbar\omega}{k_B T}} - 1)^2} \, g_L(\omega) \, d\omega$$

$$= \int_0^{\omega_D} \frac{\hbar^2 \omega^2}{k_B T^2} \frac{e^{\frac{\hbar\omega}{k_B T}}}{(e^{\frac{\hbar\omega}{k_B T}} - 1)^2} \left[\frac{1}{2\pi^2} (L_1 L_2 L_3) \frac{1}{v_L^3} \omega^2 \right] d\omega$$

$$= \frac{V}{2\pi^2} \frac{1}{v_L^3} \frac{k_B^3 T^2}{\hbar^2} \int_0^{\omega_D} \frac{\hbar^4 \omega^4}{k_B^4 T^4} \frac{e^{\frac{\hbar\omega}{k_B T}}}{(e^{\frac{\hbar\omega}{k_B T}} - 1)^2} \, d\omega$$

$$= \frac{V}{2\pi^2} \frac{1}{v_L^3} \frac{k_B^4 T^3}{\hbar^3} \int_0^{\frac{\Theta_D}{T}} \frac{x^4 e^x}{(e^x - 1)^2} \, dx$$

We know that: $N_L(\omega) = r \, N_c = \frac{1}{6} \frac{L_1 L_2 L_3}{\pi^2} \frac{\omega^3}{v_L^3}$,

Then, $\omega_D^3 = r \, N_c \frac{v_L^3 \, 6\pi^2}{V}$

And having $\frac{\hbar^3 \omega_D^3}{k_B^3} = \Theta_D^3$

So, $\Theta_{D,L}^3 = \frac{\hbar^3}{k_B^3} r \, N_c \frac{v_L^3 \, 6\pi^2}{V}$

$$C_{v,L} = 3 \, k_B r \, N_c \frac{T^3}{\Theta_{D,L}^3} \int_0^{\frac{\Theta_{D,L}}{T}} \frac{x^4 e^x}{(e^x - 1)^2} \, dx \tag{104b}$$

In a similar way,

The contribution of the torsional branch to the specific heat is

$$C_{v,T} = 3\ k_B r\ N_c\ \frac{T^3}{\Theta_{D,T}^3} \int_0^{\frac{\Theta_{D,T}}{T}} \frac{x^4 e^x}{(e^x-1)^2}\ dx \tag{104c}$$

And that of the bending phonons is represented by:

$$C_{v,B} = \int_0^{\omega_D} \frac{\hbar^2 \omega^2}{k_B T^2} \frac{e^{\frac{\hbar\omega}{k_B T}}}{(e^{\frac{\hbar\omega}{k_B T}}-1\ )^2} \frac{V}{4\pi^2} \frac{1}{c_B^{3/2}}\ \omega^{1/2} d\omega$$

$$= \frac{V}{4\pi^2} \frac{1}{c_B^{3/2}} \frac{k_B^{3/2} T^{1/2}}{\hbar^{1/2}} \int_0^{\omega_D} \frac{\hbar^{5/2} \omega^{5/2}}{k_B^{5/2} T^{5/2}} \frac{e^{\frac{\hbar\omega}{k_B T}}}{(e^{\frac{\hbar\omega}{k_B T}}-1\ )^2}\ d\omega$$

$$= \frac{3}{2}\ k_B r\ N_c\ \frac{T^{3/2}}{\Theta_{D,B}^{3/2}} \int_0^{\frac{\Theta_{D,B}}{T}} \frac{x^{5/2} e^x}{(e^x-1)^2}\ dx \quad \text{where}\ \ \Theta_{D,B}^{3/2} = \frac{\hbar^{3/2}}{k_B^{3/2}}\ r\ N_c\ \frac{c_B^{3/2}\ 6\pi^2}{V} \tag{104d}$$

2. Derivation of Θ_D as a function of Temperature

The exact specific heat is given by

$$C_v = k_B\ \sum_j \sum_k \frac{(\frac{\hbar\omega}{2k_B T})^2}{(\sinh\frac{\hbar\omega}{2k_B T})^2} \tag{105}$$

Where j stands for longitudinal, bending, and torsional branches and $\omega(k)$ can be

obtained from the dispersion relations of the modes. In order to find Debye Temperature

$\Theta_{D,L}$, $\Theta_{D,T}$ and $\Theta_{D,B}$

$$k_B \sum_k \frac{(\frac{\hbar\omega}{2k_B T})^2}{(\sinh\frac{\hbar\omega}{2k_B T})^2} = 3\ k_B r\ N_c\ \frac{T^3}{\Theta_{D,L}^3} \int_0^{\frac{\Theta_{D,L}}{T}} \frac{x^4 e^x}{(e^x-1)^2}\ dx \tag{106a}$$

$$k_B \sum_k \frac{(\frac{\hbar\omega}{2k_B T})^2}{(\sinh\frac{\hbar\omega}{2k_B T})^2} = 3\ k_B r\ N_c\ \frac{T^3}{\Theta_{D,T}^3} \int_0^{\frac{\Theta_{D,T}}{T}} \frac{x^4 e^x}{(e^x-1)^2}\ dx \tag{106b}$$

$$k_B \sum_k \frac{(\frac{\hbar\omega}{2k_B T})^2}{(\sinh\frac{\hbar\omega}{2k_B T})^2} = \frac{3}{2}\ k_B r\ N_c\ \frac{T^{3/2}}{\Theta_{D,B}^{3/2}} \int_0^{\frac{\Theta_{D,B}}{T}} \frac{x^{5/2} e^x}{(e^x-1)^2}\ dx \tag{106c}$$

And we solve for Θ_D at each temperature.

3. Derivation of the Mode Grüneisen Parameter as a function of temperature

The Grüneisen parameter γ describes how the volume change of a crystal affects the vibrational properties. It can be determined as a function of temperature by using the following formula:

$$\gamma = \frac{\sum_j \sum_k \gamma_j(k) C_v(k)}{\sum_k C_v(k)} \tag{107}$$

where $\gamma_j(k) = \frac{-\Omega}{\omega(k)} \frac{\partial \omega_j(k)}{\partial \Omega}$ (108)

Where Ω is the volume of the nanowire under study.

Since $\omega_L{}^2 = \frac{E}{\rho}\pi^2 [(\frac{n_1}{L_1})^2 + (\frac{n_2}{L_2})^2 + (\frac{n_3}{L_3})^2]$ and since the volume change of the nanowire is due to both changes in both length and the cross-sectional area of the nanowire, we can write

$$\gamma_L(k) = \frac{-L_1}{\omega_j(k)}\frac{\partial \omega_L(k)}{\partial L_1} \times \frac{-L_2}{\omega_j(k)}\frac{\partial \omega_L(k)}{\partial L_2} \times \frac{-L_3}{\omega_j(k)}\frac{\partial \omega_L(k)}{\partial L_3}$$

$$\frac{\partial \omega}{\partial L_1} = -\left(\frac{E}{\rho}\right)\frac{\pi^2 n_1^2}{L_1^3 \omega_L(k)}$$

So, $\gamma_L(k) = \left(\frac{E}{\rho}\right)\frac{\pi^2 n_1^2}{L_1^2 \omega_L^2(k)} \times \left(\frac{E}{\rho}\right)\frac{\pi^2 n_2^2}{L_2^2 \omega_L^2(k)} \times \left(\frac{E}{\rho}\right)\frac{\pi^2 n_3^2}{L_3^2 \omega_L^2(k)}$ (109)

Using a similar approach,

$$\gamma_T(k) = \left(\frac{C}{\rho I}\right)\frac{\pi^2 n_1^2}{L_1^2 \omega_T^2(k)} \times \left(\frac{C}{\rho I}\right)\frac{\pi^2 n_2^2}{L_2^2 \omega_T^2(k)} \times \left(\frac{C}{\rho I}\right)\frac{\pi^2 n_3^2}{L_3^2 \omega_T^2(k)} \tag{110}$$

$$\gamma_B(k) = \frac{8}{\omega_B^3} c_B^{3/2} \pi^6 \times \frac{n_1^2 n_2^2 n_3^2}{V^2} \tag{111}$$

At this point, the overall Grüneisen parameter γ can be obtained.

CHAPTER V

THERMAL CONDUCTIVITY OF CYLINDRICAL NANOWIRES

We present a general predictable model for the lattice thermal conductivity in cylindrical nanowires with a circular cross-section. The work accounts for modifying the model presented for pristine nanowires in cylindrical coordinates to explain the effect of the circular cross-section instead of a square one. Heat transfer in nanowires with diameters of only a few nanometers are under study. Having nanoscale dimensions in the radial direction, nanowires exhibit size confinement effects, induced by the boundaries that give them different physical properties as compared to bulk crystals. With no azimuthal dependence of the phonon distribution function, the two-dimensional geometry (r and z) of the rod simplifies the calculations. In a similar manner, the dispersion relations along with the boundary scattering rate and the crystal vibrational parameters are derived in cylindrical coordinates and employed later in the lattice thermal conductivity formalism.

A. Dispersion Relations and Allowable Normal Modes

On an attempt to find the allowable wave vectors for the phonon dispersion of a cylindrical nanowire, we planned a usual approach in solving the equations of motion of the solid under study in cylindrical coordinates taking into account the convenient boundary conditions for obtaining a simple solution.

The equations of motion of a solid are:

$$\rho \, \frac{\partial^2 U}{\partial t^2} = \mu \, \nabla^2 U + (\lambda + \mu) \, \nabla \, (\nabla . U) \tag{112}$$

51

where ρ is the density of the solid, μ and λ are Lame constants. U is the displacement of a point in the solid. For the boundary conditions, we will assume that we have azimuthal symmetry and that at the boundary of the nanowire (r =R) the radial component of the displacement blows up to zero along with the derivative of the z-component with respect to the radial one. With the above assumptions, and solving the equation of motion in cylindrical coordinates by the separation of variable technique, the displacement of a point in a nanowire is described as

$$U(r, z, t) = J_m \left(\frac{z_m.r}{R}\right) \cos(n\Theta) \sin\left(\frac{n_3\pi z}{L}\right) e^{-i\omega t} \tag{113}$$

This is the polar analogous to

$$U(x, y, z, t) = \sin\left(\frac{n_1\pi x}{L_1}\right) \sin\left(\frac{n_2\pi x}{L_2}\right) \sin\left(\frac{n_3\pi x}{L_3}\right) e^{-i\omega t} \tag{114}$$

where the zeros of the sine function are replaced by the zeros of the Bessel's function z_m. The radial component in the cylindrical coordinates involves a solution in terms of Bessel's function. Note that at the boundary of the wire i.e. r=R, $J_m (z_m)$ drops to zero. Ignoring the angular term i.e. azimuthal symmetry, the displacement of a point in a nanowire is

$$U(r, z, t) = J_m \left(\frac{z_m r}{R}\right) \sin\left(\frac{n_3\pi z}{L}\right) e^{-i\omega t} \tag{115}$$

On substituting this solution in the equation of motion above, we obtain the basic equation for determining the normal mode frequencies:

$$\left[\frac{\rho\omega^2}{\pi^2} - (\lambda + 2\mu)\left[\left(\frac{z_m}{\pi R}\right)^2 + \left(\frac{n_3}{L}\right)^2\right]\right]\left[\frac{\rho\omega^2}{\pi^2} - \mu\left[\left(\frac{z_m}{\pi R}\right)^2 + \left(\frac{n_3}{L}\right)^2\right]\right] = 0 \tag{116}$$

The solutions of the equation above are:

$$\omega_L^2 = \frac{E}{\rho}\pi^2 \left[\left(\frac{z_m}{\pi R}\right)^2 + \left(\frac{n_3}{L}\right)^2\right] \tag{117}$$

$$\omega_B^2 = \frac{E I_{x,y}}{\rho S}\pi^4 \left[\left(\frac{z_m}{\pi R}\right)^2 + \left(\frac{n_3}{L}\right)^2\right]^2 \tag{118}$$

52

$$\omega_T^2 = \frac{C}{\rho I}\pi^2 \left[\left(\frac{z_m}{\pi R}\right)^2 + \left(\frac{n_3}{L}\right)^2 \right] \tag{119}$$

where L, B and T refers to longitudinal, bending and torsional branches.

B. Phonon Distribution Function

Assuming a temperature gradient along the z-direction, the distribution function for phonons in a pristine nanowire has an explicit dependence on *x* and *y*. The corresponding Boltzmann equation is

$$v_z \frac{dN}{dT}\frac{\partial T}{\partial z} + v_x \frac{\partial N}{\partial x} + v_y \frac{\partial N}{\partial y} + N\tau = 0 \tag{120}$$

With

$$N = \frac{P\tau}{2}\left[(1 - \exp\left(\frac{-x(y)}{\tau v_x}\right)) + (1 - \exp\left(\frac{-y(x)}{\tau v_y}\right)) \right] + \sigma_z \exp\left(\frac{-x(y)}{\tau v_x}\right) + \sigma_z \exp\left(\frac{-y(x)}{\tau v_y}\right)] \tag{121}$$

where P= $v_z \frac{dN}{dt}\frac{\partial T}{\partial z}$ is the negative of the rate at which phonons are delivered to a unit volume of the reciprocal space [29]. The above distribution function is a solution of the Boltzmann equation for any cross section dimensions and shape.

In the case of a nanowire with a circular cross section and with a temperature gradient aligned parallel to the rod axis in the *z* direction, the phonon distribution function deviates from equilibrium. The thermal gradient pumps the phonons in the *z* direction to every point of the cross section of the nanowire. For small deviations from equilibrium, the temperature gradient is assumed to depend on *z* only. With cylindrical coordinates (r, Φ, z) imposed on the system and considering azimuthal symmetry, the distribution function N has an explicit *r* dependence, with an implicit dependence on *z* through the temperature gradient:

$$N = P\,\tau\left[1 - \frac{r}{R}e^{\frac{-(R-r)}{\tau v_B}}\right] + \sigma\frac{r}{R}e^{\frac{-(R-r)}{\tau v_B}} \tag{122}$$

53

Where τ is the total relaxation time associated with all the resistive processes and σ determines the deviation in the phonon distribution function at the boundary. In the very vicinity of the boundary, $R = r$, there is thermalization, which means that the phonon distribution function is a constant σ and is determined by the interaction between volume phonons and surface phonons. In infinite radial direction, big enough R, N restores back to Pτ as if we are dealing with a bulk material with no spatial dependence of the phonon distribution function.

C. Derivation of the Phonon-Boundary Scattering Rate

Using the expression of the phonon distribution function derived in the previous section, the boundary scattering rate is

$$\frac{1}{\tau_B} = \frac{\iint v\, \partial N/\partial r\, dS}{\iint N\, dS} \tag{123}$$

Where dS is the differential cross-sectional area. We can now derive the rates at which phonons scatter by the boundaries as the following:

$$\frac{\partial N}{\partial r} = -\,P\tau\,\frac{r}{R}\exp\left(\frac{-R}{\tau v_B}\right)\frac{1}{\tau v_B}\exp\left(\frac{r}{\tau v_B}\right) - P\tau\,\frac{1}{R}\exp\left(\frac{-(R-r)}{\tau v_B}\right) + \sigma\,\frac{r}{R}\exp\left(\frac{-R}{\tau v_B}\right)\frac{1}{\tau v_B}\exp\left(\frac{r}{\tau v_B}\right) +$$

$$\sigma\,\frac{1}{R}\exp\left(\frac{-(R-r)}{\tau v_B}\right) \tag{124}$$

And

$$\int \frac{\partial N}{\partial r}\, dS = (-\,P\tau + \sigma\,)\,\frac{1}{R}\exp\left(\frac{-R}{\tau v_B}\right)\int \exp\left(\frac{r}{\tau v_B}\right)dS + \frac{(-P+\frac{\sigma}{\tau})}{Rv_B}\exp\left(\frac{-R}{\tau v_B}\right)\int r\exp\left(\frac{r}{\tau v_B}\right)dS$$

$$= \frac{(-\,P\tau + \sigma)}{R}\,\exp\left(\frac{-R}{\tau v_B}\right)\int_0^R 2\pi r\,\exp\left(\frac{r}{\tau v_B}\right)dr + \frac{(-P+\frac{\sigma}{\tau})}{Rv_B}\exp\left(\frac{-R}{\tau v_B}\right)\int_0^R 2\pi r^2\exp\left(\frac{r}{\tau v_B}\right)dr$$

$$= 2\pi\,\frac{(-\,P\tau + \sigma)}{R}\exp\left(\frac{-R}{\tau v_B}\right)[\tau^2 v_B^2 + R\tau v_B\exp\left(\frac{R}{\tau v_B}\right) - \tau^2 v_B^2\exp\left(\frac{R}{\tau v_B}\right)] + \frac{(-P+\frac{\sigma}{\tau})}{Rv_B}\exp\left(\frac{-R}{\tau v_B}\right)$$

$$[2\tau^3 v_B^3\exp\left(\frac{R}{\tau v_B}\right) + R^2\tau v_B\exp\left(\frac{R}{\tau v_B}\right) - 2R\tau^2 v_B^2\exp\left(\frac{R}{\tau v_B}\right) - 2\tau^3 v_B^3] \tag{125}$$

54

And computing $\int N \, dS$

$$\int N \, dS = \int P\tau \, dS - P\frac{\tau}{R}\exp\left(\frac{-R}{\tau v_B}\right)\int r \exp\left(\frac{-r}{\tau v_B}\right) dS + \frac{\sigma}{R}\exp\left(\frac{-R}{\tau v_B}\right)\int r \exp\left(\frac{R}{\tau v_B}\right) dS \qquad (126)$$

$$= 2\pi P\tau \int_0^R r \, dr - \frac{2\pi P\tau}{R}\exp\left(\frac{-R}{\tau v_B}\right)\int_0^R r^2 \, exp\left(\frac{r}{\tau v_B}\right) dR + \frac{2\pi\sigma}{R}\left(\frac{-R}{\tau v_B}\right)\int r^2 exp\left(\frac{r}{\tau v_B}\right) dr$$

Note here that P is the negative of the rate at which phonons are delivered to a unit volume of the reciprocal lattice and r is the variable cross-section radius varying between 0 and R (where R is the nanowire radius).

Dividing equation (125) by equation (126) and performing some simplifications and arrangements, we get the phonon boundary scattering rates in a cylindrical nanowire of a circular cross-section:

$$\frac{1}{\tau_B} = \frac{v_B}{R} \cdot \frac{\left[-\tau v_B R + \tau^2 v_B^2 + 3\tau^2 v_B^2 exp\left(\frac{-R}{\tau v_B}\right) + R^2\right]\left[1 - \frac{\sigma}{P\tau}\right]}{R^2 - \left[\tau v_B R - 2\tau^2 v_B^2 + \frac{2\tau^3 v_B^3}{R} - \frac{2\tau^3 v_B^3}{R}exp\left(\frac{-R}{\tau v_B}\right)\right]\left[1 - \frac{\sigma}{P\tau}\right]} \qquad (127)$$

To evaluate this rate, we need to estimate a magnitude for the term $\frac{\sigma}{P\tau}$. As a phonon strikes a boundary, it can undergo transmission, specular reflection or diffuse scattering with a random change of its propagation direction. In the case of surfaces, only reflection or backward scattering can take place, whereas for interfaces, transmission is also possible. The probabilities for a phonon to reflect, transmit or scatter at a surface or interface strongly depend on the characteristics of the sample boundary. A good understanding of the phonon dynamics at the surface provides a clear picture of phonon-boundary interactions and their effect on the thermal transport. Examining the expression of the phonon distribution function in the case of a cylindrical nanowire of a circular cross-section,

$$N = P\tau \left[1 - \frac{r}{R} e^{\frac{-(R-r)}{\tau v_B}}\right] + \sigma \frac{r}{R} e^{\frac{-(R-r)}{\tau v_B}}$$

In the case of completely diffusive boundaries, σ is equal to zero. While, in the case of

total specular phonon reflection, $P\tau$ must be remain equal to σ to ensure that N reduces

to τP at any position in the rod. However, in the case of partial specular phonon

reflection, the ratio of σ to τP must be equal to a positive constant smaller than one so

that N reduces fast to τP as the phonons move away from the boundaries of the

nanowire. Thus, the term $\frac{\sigma}{P\tau}$ employed in the phonon boundary scattering rates is always

independent of the position in the crystal and has a magnitude between zero and one. As

mentioned earlier, roughness plays an important role in phonon dynamics at the surface.

Surface irregularities reduce the lifetime of a surface phonon and consequently reduce

σ. Therefore, the term $\frac{\sigma}{P\tau}$ has all the characteristics of the phonon specularity factor. The

phonon specularity factor, which was originally derived by Ziman, depends on the

characteristics of the incident phonon and surface asperities according to

$$p = \exp\left(-16\pi^2\lambda^2\omega^2/v^2\right) \tag{128}$$

Where λ is the root mean square (rms) surface irregularity.

D. Density of States

We can now calculate the function g (ω), the fraction of normal modes with

frequencies in the interval (ω, ω+dω). The number of longitudinal modes with

frequencies less than ω is the number of positive integer lattice points (z_m and n_3)

which obey:

$$\pi^2 v_L^2 \left[\left(\frac{z_m}{\pi R}\right)^2 + \left(\frac{n_3}{L}\right)^2\right] \le \omega^2 \tag{129}$$

that is, the number of lattice points lying within an octant of the ellipse specified by:

$$\frac{x^2}{\pi^2 R^2} + \frac{y^2}{L^2} = \frac{\omega^2}{\pi 2\, v_L^2} \tag{130}$$

To a first approximation, in the limit of a thick nanowire, this number is equal to the area in the

$$\frac{\pi^2 v_l^2}{\pi^2 R^2 \omega} x^2 + \frac{\pi^2 v_L^2}{L^2 \omega^2} y^2 = 1$$

Implies that
$$\frac{x^2}{\frac{R^2 \omega^2}{v_L^2}} + \frac{y^2}{\frac{L^2 \omega^2}{\pi^2 v_L^2}} = 1 \tag{131}$$

$N_L(\omega) = \frac{\pi}{4}\, a\, b \quad$ where $a = \frac{R^2 \omega^2}{v_L^2}$ and $b = \frac{L^2 \omega^2}{\pi^2 v_L^2}$

$$N_L(\omega) = \frac{R\, L\, \omega^2}{4\, v_L^2} \tag{132}$$

With a similar approach, we can find that the number of torsional modes of frequencies less than ω and is given by

$$N_T(\omega) = \frac{R\, L\, \omega^2}{4\, v_T^2} \tag{133}$$

The number of bending modes with frequencies less than ω is the number of positive integer lattice points (z_m and n) which obey:

$$\pi^4\, v_B^2\, [(\tfrac{z_m}{\pi R})^2 + (\tfrac{n_3}{L})^{2]2} \le \omega^2 \tag{134}$$

Implies that

$$\pi^4\, v_B^2\, [(\tfrac{z_m^2}{\pi^2 R^2})^2 + (\tfrac{n_3^2}{L^2})^2 + \tfrac{2 z_m^2 n_3^2}{\pi^2 R^2 L^2}\,] \le \omega^2$$

$$\leftrightarrow [(\tfrac{z_m^2}{\pi^2 R^2})^2 + (\tfrac{n_3^2}{L^2})^2 + \tfrac{2 z_m^2 n_3^2}{\pi^2 R^2 L^2}\,] \le \frac{\omega^2}{\pi^4 v_B^2}$$

$$\leftrightarrow \frac{\pi^4 v_B^2}{\omega^2 \pi^4 R^4} x^2 + \frac{\pi^4 v_B^2}{\omega^2 L^2} y^2 + \frac{2\pi^4 v_B^2}{\omega^2 \pi^2 R^2 L^2} z^2 = 1$$

57

$$\leftrightarrow \frac{x^2}{\frac{\omega^2 R^4}{v_B^2}} + \frac{y^2}{\frac{\omega^2 L^4}{\pi^4 v_B^2}} + \frac{z^2}{\frac{\omega^2 R^2 L^2}{2\pi^2 v_B^2}} = 1 \tag{135}$$

With $N_B(\omega) = \frac{1}{8} \times \frac{4}{3} \pi$ a b c

$$N_B(\omega) = \frac{R^3 L^3}{6\sqrt{2}\pi^2} \times \frac{\omega^3}{v_B^3} \tag{136}$$

The total number of modes with frequencies less than ω is thus

$$N(\omega) = N_L(\omega) + N_T(\omega) + N_B(\omega)$$

$$= \frac{RL}{4}\left(\frac{1}{v_L^2} + \frac{1}{v_T^2}\right)\omega^2 + \frac{R^3 L^3}{6\sqrt{2}\pi^2}\frac{\omega^3}{v_B^3} \tag{137}$$

If we consider a single dispersion relation with a cut-off frequency ω_D, we can say that the total number of modes is

$$N(\omega) = \frac{RL}{4}\left(\frac{1}{v_L^2} + \frac{1}{v_T^2}\right)\omega_D^2 + \frac{R^3 L^3}{6\sqrt{2}\pi^2}\frac{\omega_D^3}{v_B^3} \tag{138}$$

On the other hand, $N(\omega) = 3rN_c$ where r is the number of atoms in the unit cell and N_c is the number of unit cells in the nanowire

$$3rN_c = \frac{RL}{4}\left(\frac{1}{v_L^2} + \frac{1}{v_T^2}\right)\omega_D^2 + \frac{R^3 L^3}{6\sqrt{2}\pi^2}\frac{\omega_D^3}{v_B^3} \tag{139}$$

From its definition, we know that the density of states is given in terms of $N(\omega)$ by the relation:

$$g(\omega)\,d\omega = \frac{1}{3rN_c}[N(\omega+d\omega) - N(\omega)] = \frac{1}{3rN_c}N'(\omega)\,d\omega$$

$$= \frac{1}{3rN_c}\left[\frac{RL}{2}\left(\frac{1}{v_L^2} + \frac{1}{v_T^2}\right)\omega + \frac{R^3 L^3}{2\sqrt{2}\pi^2}\frac{\omega^2}{v_B^3}\right] \tag{140}$$

E. Formalism for the Lattice Thermal Conductivity in a Cylindrical Nanowire

The lattice thermal conductivity in the nanowire is given by

$$K = -V \sum_k \hbar\omega \, \widetilde{N} \frac{v_L}{\nabla T} \tag{141}$$

Where V is the volume of the first Brillouin zone, and thus

$$K = - \int_0^{\omega_D} \hbar\omega \, \widetilde{N} \frac{v_L}{\nabla T} \, g\,(\omega) \, d\omega \tag{142}$$

Introducing the expression of the phonon density of states derived previously, the thermal conductivity expression reduces to

$$K = - \int_0^{\omega_D} \hbar\omega \, \widetilde{N} \frac{v_L}{\nabla T} \frac{1}{3rN_c} \left[\frac{RL}{2} \left(\frac{1}{v_L^2} + \frac{1}{v_T^2} \right) \omega + \frac{R^3 L^3}{2\sqrt{2}\pi^2} \frac{\omega^2}{v_B^3} \right] d\omega$$

$$= \frac{-v_L \, R \, L}{6rN_c} \left(\frac{1}{v_L^2} + \frac{1}{v_T^2} \right) \int_0^{\omega_D} \hbar\omega^2 \frac{\widetilde{N}}{\nabla T} \, d\omega - \frac{v_L R^3 L^3}{6\sqrt{2}rN_c\pi^2} \frac{1}{v_B^3} \int_0^{\omega_D} \hbar\omega^3 \frac{\widetilde{N}}{\nabla T} \, d\omega \tag{143}$$

The overall thermal conductivity can be seen as the sum of two conductivities; The first one is the thermal conductivity due to surface contribution described by an ellipse of area proportional to RL and the second term is the thermal conductivity due to the volume contribution described by an ellipsoid of volume proportional to R^3L^3. Equation (143) needs the expression of $\widetilde{N}$ to be solved.

1. Derivation of the Deviated Phonon Distribution Function

In order to find $\widetilde{N}$, we follow Callaway's procedure. We know that the original Boltzmann equation is:

$$-v_L \frac{\partial N}{\partial z} - v_r \frac{\partial N}{\partial r} + \frac{N_u - N}{\tau_N} + \frac{\overline{N} - N}{\tau_{U+I}} = 0 \tag{144}$$

Moreover, it can be written as:

$$-v_L \frac{\partial N}{\partial z} + \frac{N_u - N}{\tau_N} + \frac{\bar{N} - N}{\tau_R} = 0 \tag{145}$$

Where $\frac{1}{\tau_R} = \frac{1}{\tau_U} + \frac{1}{\tau_I} + \frac{1}{\tau_B}$, and since $N = \bar{N} + \tilde{N}$, we can write Boltzmann equation in the form:

$$-v_L \frac{d\bar{N}}{dT} \frac{\partial T}{\partial z} + \frac{N_u - N}{\tau_N} - \frac{\tilde{N}}{\tau_R} = 0 \tag{146}$$

On the other hand,

$$N_u = \bar{N} + \frac{\vec{u}.\vec{k_z}}{k_B T} \frac{e^{\frac{\hbar\omega}{k_B T}}}{(e^{\frac{\hbar\omega}{k_B T}} - 1)^2} \tag{147}$$

Where N_u is the displaced phonon distribution function due to normal processes and $\vec{u}$ is a vector having the dimensions of energy x length describing the displacement of Planck distribution and $\vec{k_z}$ is a wave vector in the z-direction i.e. the direction of temperature gradient. Substituting equation (147) in (146), we get

$$-v_L \left[\frac{\hbar\omega}{k_B T^2} \frac{e^{\frac{\hbar\omega}{k_B T}}}{(e^{\frac{\hbar\omega}{k_B T}} - 1)^2}\right] \frac{\partial T}{\partial z} + \frac{1}{\tau_N} \left[\bar{N} + \frac{\vec{u}.\vec{k_z}}{k_B T} \frac{e^{\frac{\hbar\omega}{k_B T}}}{(e^{\frac{\hbar\omega}{k_B T}} - 1)^2} - N\right] - \frac{\tilde{N}}{\tau_R} = 0 \tag{148}$$

Through some simplifications, Boltzmann equation reduces to

$$-v_L \left[\frac{\hbar\omega}{k_B T^2} \frac{e^{\frac{\hbar\omega}{k_B T}}}{(e^{\frac{\hbar\omega}{k_B T}} - 1)^2}\right] \frac{\partial T}{\partial z} + \frac{1}{\tau_N} \frac{\vec{u}.\vec{k_z}}{k_B T} \frac{e^{\frac{\hbar\omega}{k_B T}}}{(e^{\frac{\hbar\omega}{k_B T}} - 1)^2} - \left(\frac{1}{\tau_R} + \frac{1}{\tau_N}\right) \tilde{N} = 0 \tag{149}$$

The combined relaxation time defined as:

$$\frac{1}{\tau_c} = \frac{1}{\tau_N} + \frac{1}{\tau_R} \tag{150}$$

With
$$\tilde{N} = -\alpha \, v_L \frac{\partial T}{\partial z} \frac{\hbar\omega}{k_B T^2} \frac{e^{\frac{\hbar\omega}{k_B T}}}{(e^{\frac{\hbar\omega}{k_B T}} - 1)^2} \tag{151}$$

Where α has the dimensions of a relaxation time. Substituting (151) and (150) in (149),

$$-v_L \frac{\hbar\omega}{k_B T^2} \frac{e^{\frac{\hbar\omega}{k_B T}}}{(e^{\frac{\hbar\omega}{k_B T}}-1\ )^2} \frac{\partial T}{\partial z} + \frac{1}{\tau_N} \frac{\vec{u}.\overrightarrow{k_z}}{k_B T} \frac{e^{\frac{\hbar\omega}{k_B T}}}{(e^{\frac{\hbar\omega}{k_B T}}-1\ )^2} - \frac{1}{\tau_c}\left[-\alpha\ v_L \frac{\partial T}{\partial z} \frac{\hbar\omega}{k_B T^2} \frac{e^{\frac{\hbar\omega}{k_B T}}}{(e^{\frac{\hbar\omega}{k_B T}}-1\ )^2}\right] = 0$$

This equation simplifies to:

$$\frac{\vec{u}.\overrightarrow{k_z}}{\tau_N} + \frac{\alpha v_L}{\tau_c} \frac{\partial T}{\partial z} \frac{\hbar\omega}{T} = v_L \frac{\hbar\omega}{T} \frac{\partial T}{\partial z} \tag{152}$$

Since $\vec{u}$ is a constant vector in the direction of temperature gradient, we can express it as

$$\vec{u} = -\frac{\hbar}{T}\ \beta\ v_L^2 \frac{\partial T}{\partial z}\ \hat{z} \tag{153}$$

Where β has the dimension of a relaxation time and $k_z = \frac{\omega}{v_L}$.

Equation (152) can be written as:

$$\alpha = \tau_c\ (1+\frac{\beta}{\tau_N}) \tag{154}$$

At this stage, we need to find β. That is why we make use of the fact that the normal processes conserve the crystal momentum. Thus, the rate of change of the total phonon momentum due to normal processes must be set equal to zero:

$$\sum_k (\frac{\partial N}{\partial t})_N . \vec{K} = 0 \tag{155}$$

Implies that

$$\int_0^{\omega_D} (\frac{\partial N}{\partial t})_N . \vec{K}\ g(\omega)d\omega$$

$$= \int_0^{\omega_D} \frac{1}{\tau_N} [\bar{N} + \frac{1}{k_B T}\ (\frac{-\hbar\omega}{T} \beta v_L \frac{\partial T}{\partial z}) \frac{e^{\frac{\hbar\omega}{k_B T}}}{(e^{\frac{\hbar\omega}{k_B T}}-1\ )^2} - N].\vec{K}\ g(\omega)\ d\omega = 0 \tag{156}$$

With $N - \bar{N} = \tilde{N}$

$$= \int_0^{\omega_D} \frac{e^{\frac{\hbar\omega}{k_B T}}}{(e^{\frac{\hbar\omega}{k_B T}}-1\ )^2} \ [\frac{-\hbar\omega}{k_B T^2}\beta v_L \frac{\partial T}{\partial z}) + v_L \frac{\partial T}{\partial z}\frac{\hbar\omega}{k_B T^2}] \ \frac{\vec{K}}{\tau_N} \ g\left(\omega\right) \ d\omega = 0$$

$$= \int_0^{\omega_D} \frac{e^{\frac{\hbar\omega}{k_B T}}}{(e^{\frac{\hbar\omega}{k_B T}}-1\ )^2} \ \frac{\hbar\omega}{k_B T^2}\left(\alpha - \beta\right) \frac{\vec{K}}{\tau_N} \ g\left(\omega\right) \ d\omega = 0$$

$$= \int_0^{\omega_D} \frac{e^{\frac{\hbar\omega}{k_B T}}}{(e^{\frac{\hbar\omega}{k_B T}}-1\ )^2} \ \frac{\hbar\omega}{k_B T^2}\left(\tau_c\left(1 + \frac{\beta}{\tau_N}\right) - \beta\right) \frac{\vec{K}}{\tau_N} \ g\left(\omega\right) \ d\omega = 0$$

$$= \int_0^{\omega_D} \frac{e^{\frac{\hbar\omega}{k_B T}}}{(e^{\frac{\hbar\omega}{k_B T}}-1\ )^2} \ \frac{\hbar\omega}{k_B T^2}\tau_c \frac{\vec{K}}{\tau_N} \ g\left(\omega\right) \ d\omega + \beta \int_0^{\omega_D} \frac{e^{\frac{\hbar\omega}{k_B T}}}{(e^{\frac{\hbar\omega}{k_B T}}-1\ )^2} \ \frac{\hbar\omega}{k_B T^2}\left(\frac{\tau_c}{\tau_N} - 1\right) \frac{\vec{K}}{\tau_N} \ g\left(\omega\right) \ d\omega = 0$$

So,

$$\beta = \frac{\int_0^{\omega_D} \frac{e^{\frac{\hbar\omega}{k_B T}}}{(e^{\frac{\hbar\omega}{k_B T}}-1\ )^2} \ \frac{\hbar\omega}{k_B T^2}\tau_c \frac{\vec{K}}{\tau_N} \ g(\omega) \ d\omega}{\int_0^{\omega_D} \frac{e^{\frac{\hbar\omega}{k_B T}}}{(e^{\frac{\hbar\omega}{k_B T}}-1\ )^2} \ \frac{\hbar\omega}{k_B T^2}(\frac{\tau_c}{\tau_N}-1)\frac{\vec{K}}{\tau_N} \ g(\omega) d\omega} \tag{157}$$

With

$$\vec{K}.g\left(\omega\right) = \tfrac{1}{3} \ [\frac{\omega}{v_L} + \frac{\omega}{v_T} + \sqrt{\frac{\omega}{v_B}} \ ] \times \frac{1}{3rN_c} \ [\frac{RL}{2} \ (\frac{1}{v_L^2} + \frac{1}{v_T^2})\ \omega + \frac{R^3 L^3}{2\sqrt{2}\pi^2}\frac{\omega^2}{v_B^3} \ ]$$

$$= \frac{1}{9rN_c} \ [\frac{RL}{2} \ (\frac{1}{v_L^2} + \frac{1}{v_T^2})\ (\frac{\omega^2}{v_L} + \frac{\omega^2}{v_T} + \frac{\omega^{3/2}}{\sqrt{v_B}}) + \frac{R^3 L^3}{2\sqrt{2}\pi^2}\frac{1}{v_B^3} \ (\frac{\omega^3}{v_L} + \frac{\omega^3}{v_T} + \frac{\omega^{5/2}}{\sqrt{v_B}})] \tag{158}$$

Finally,

$$K = \frac{v_L R L}{6rN_c} \ (\frac{1}{v_L^2} + \frac{1}{v_T^2}) \int_0^{\omega_D} \hbar\omega^2 \ \tau_c \ (1 + \frac{\beta}{\tau_N}) \ v_L \ \frac{\hbar\omega}{k_B T^2}\frac{e^{\frac{\hbar\omega}{k_B T}}}{(e^{\frac{\hbar\omega}{k_B T}}-1\ )^2} \ d\omega + \frac{v_L R^3 L^3}{6\sqrt{2}rN_c\pi^2} \ \frac{1}{v_B^3} \int_0^{\omega_D} \hbar\omega^3 \ \tau_c$$

$$(1 + \frac{\beta}{\tau_N}) \ v_L \ \frac{\hbar\omega}{k_B T^2}\frac{e^{\frac{\hbar\omega}{k_B T}}}{(e^{\frac{\hbar\omega}{k_B T}}-1\ )^2} \ d\omega$$

$$= \frac{v_L^2\,R\,L}{6rN_c}\left(\frac{1}{v_L^2}+\frac{1}{v_T^2}\right)\left[\int_0^{\omega_D}\hbar\omega^2\,\tau_c\,\frac{\hbar\omega}{k_BT^2}\frac{e^{\frac{\hbar\omega}{k_BT}}}{(e^{\frac{\hbar\omega}{k_BT}}-1\ )^2}\,d\omega+\beta\int_0^{\omega_D}\hbar\omega^2\,\frac{\tau_c}{\tau_N}\frac{\hbar\omega}{k_BT^2}\frac{e^{\frac{\hbar\omega}{k_BT}}}{(e^{\frac{\hbar\omega}{k_BT}}-1\ )^2}\,d\omega\right]+$$

$$\frac{v_L^2 R^3L^3}{6\sqrt{2r}N_c\pi^2}\frac{1}{v_B^3}\left[\int_0^{\omega_D}\hbar\omega^3\,\tau_c\,\frac{\hbar\omega}{k_BT^2}\frac{e^{\frac{\hbar\omega}{k_BT}}}{(e^{\frac{\hbar\omega}{k_BT}}-1\ )^2}\,d\omega+\beta\int_0^{\omega_D}\hbar\omega^3\,\frac{\tau_c}{\tau_N}\frac{\hbar\omega}{k_BT^2}\frac{e^{\frac{\hbar\omega}{k_BT}}}{(e^{\frac{\hbar\omega}{k_BT}}-1\ )^2}\,d\omega\right] \quad (159)$$

With $x=\frac{\hbar\omega}{k_BT}$, $dx=\frac{\hbar}{k_BT}\,d\omega$

$$K=\frac{v_L^2\,R\,L}{6rN_c}\left(\frac{1}{v_L^2}+\frac{1}{v_T^2}\right)\left[\frac{k_B^3T^2}{\hbar^2}\int_0^{\frac{\Theta_D}{T}}\tau_c\,\frac{x^3e^x}{(e^x-1)^2}\,dx+\beta\,\frac{k_B^3T^2}{\hbar^2}\int_0^{\frac{\Theta_D}{T}}\frac{\tau_c}{\tau_N}\frac{x^3e^x}{(e^x-1)^2}\,dx\right]++\frac{v_L^2R^3L^3}{6\sqrt{2r}N_c\pi^2}\frac{1}{v_B^3}$$

$$\left[\frac{k_B^4T^3}{\hbar^3}\int_0^{\frac{\Theta_D}{T}}\tau_c\,\frac{x^4e^x}{(e^x-1)^2}\,dx+\beta\,\frac{k_B^4\,T^3}{\hbar^3}\int_0^{\frac{\Theta_D}{T}}\frac{\tau_c}{\tau_N}\frac{x^4e^x}{(e^x-1)^2}\,dx\right]$$

$$K=\frac{v_L^2\,R\,L}{6rN_c}\left(\frac{1}{v_L^2}+\frac{1}{v_T^2}\right)\frac{k_B^3T^2}{\hbar^2}\left[\int_0^{\frac{\Theta_D}{T}}\tau_c\,\frac{x^3e^x}{(e^x-1)^2}\,dx+\beta\int_0^{\frac{\Theta_D}{T}}\frac{\tau_c}{\tau_N}\frac{x^3e^x}{(e^x-1)^2}\,dx\right]++\frac{v_L^2R^3L^3}{6\sqrt{2r}N_c\pi^2}\frac{1}{v_B^3}\frac{k_B^4\,T^3}{\hbar^3}$$

$$\left[\int_0^{\frac{\Theta_D}{T}}\tau_c\,\frac{x^4e^x}{(e^x-1)^2}\,dx+\beta\int_0^{\frac{\Theta_D}{T}}\frac{\tau_c}{\tau_N}\frac{x^4e^x}{(e^x-1)^2}\,dx\right] \quad (160)$$

The result above shows 3 terms, the first two with a square dependence on temperature and the other with a cubic one. The first one corresponds to the contribution of longitudinal phonons with no significance about the nature of the material. The second term corresponds to torsional phonons with also no significance about the material having the ratio of longitudinal speed to the torsional one very close i.e.almost one. As the radius of the nanowire is big enough the last term dominates eq. (160) and the first two terms vanish, and when the nanowire radius gets very small the thermal conductivity expression is determined by the first two terms. This generalizes that at very small radius, the nanowire can be treated as a one-dimensional axial wire and that all nanowires with very small radii have the same thermal conductivity.

F. Derivation of the Crystal Vibrational Parameters

1. Specific Heat and Debye Temperature

The total energy associated with the nanowire normal modes can be written as

$$E = \sum_k \left(\frac{\hbar\omega}{2} + \frac{\hbar\omega}{e^{\frac{\hbar\omega}{k_BT}} - 1} \right) \tag{161}$$

The specific heat is given by:

$$C_v = \frac{\partial E}{\partial T}$$

$$= \sum_k \frac{\partial}{\partial T} \left(\frac{\hbar\omega}{e^{\frac{\hbar\omega}{k_BT}} - 1} \right)$$

$$= \sum_k \frac{\hbar^2\omega^2}{k_BT^2} \frac{e^{\frac{\hbar\omega}{k_BT}}}{(e^{\frac{\hbar\omega}{k_BT}} - 1)^2}$$

$$= \int_0^{\omega_D} \frac{\hbar^2\omega^2}{k_BT^2} \frac{e^{\frac{\hbar\omega}{k_BT}}}{(e^{\frac{\hbar\omega}{k_BT}} - 1)^2} \, g(\omega) \, d\omega \tag{162}$$

$$= \int_0^{\omega_D} \frac{\hbar^2\omega^2}{k_BT^2} \frac{e^{\frac{\hbar\omega}{k_BT}}}{(e^{\frac{\hbar\omega}{k_BT}} - 1)^2} \left\{ \frac{1}{3rN_c} \left[\frac{RL}{2} \left(\frac{1}{v_L^2} + \frac{1}{v_T^2} \right) \omega + \frac{R^3L^3}{2\sqrt{2}\pi^2} \frac{\omega^2}{v_B^3} \right] \right\} d\omega$$

$$= \frac{1}{3rN_c} \int_0^{\omega_D} \frac{\hbar^2\omega^2}{k_BT^2} \frac{e^{\frac{\hbar\omega}{k_BT}}}{(e^{\frac{\hbar\omega}{k_BT}} - 1)^2} \frac{RL}{2} \left(\frac{1}{v_L^2} + \frac{1}{v_T^2} \right) \omega \, d\omega + \frac{1}{3rN_c} \int_0^{\omega_D} \frac{\hbar^2\omega^2}{k_BT^2} \frac{e^{\frac{\hbar\omega}{k_BT}}}{(e^{\frac{\hbar\omega}{k_BT}} - 1)^2} \frac{R^3L^3}{2\sqrt{2}\pi^2} \frac{\omega^2}{v_B^3} \, d\omega$$

$$= \frac{RL}{6rN_c} \left(\frac{1}{v_L^2} + \frac{1}{v_T^2} \right) \frac{k_B^2 T}{\hbar} \int_0^{\omega_D} \frac{\hbar^3\omega^3}{k_B^3 T^3} \frac{e^{\frac{\hbar\omega}{k_BT}}}{(e^{\frac{\hbar\omega}{k_BT}} - 1)^2} \, d\omega + \frac{R^3L^3}{6\sqrt{2}\pi^2 rN_c} \frac{1}{v_B^3} \frac{k_B^3 T^2}{\hbar^2} \int_0^{\omega_D} \frac{\hbar^4\omega^4}{k_B^4 T^4} \frac{e^{\frac{\hbar\omega}{k_BT}}}{(e^{\frac{\hbar\omega}{k_BT}} - 1)^2} \, d\omega$$

Change of variable $x = \frac{\hbar\omega}{k_BT}$ then $dx = \frac{\hbar}{k_BT} \, d\omega$ and $d\omega = \frac{k_BT}{\hbar} \, dx$ and $x_D = \frac{\hbar\omega_D}{k_BT} = \frac{\Theta_D}{T}$

$$C_v = \frac{RL}{6rN_c} \left(\frac{1}{v_L^2} + \frac{1}{v_T^2} \right) \frac{k_B^3 T^2}{\hbar^2} \int_0^{\frac{\Theta_D}{T}} \frac{x^3 e^x}{(e^x-1)^2} \, dx + \frac{R^3L^3}{6\sqrt{2}\pi^2 rN_c} \frac{1}{v_B^3} \frac{k_B^4 T^3}{\hbar^3} \int_0^{\frac{\Theta_D}{T}} \frac{x^4 e^x}{(e^x-1)^2} \, dx \tag{163}$$

2. Derivation of Θ_D as a function of Temperature

The exact specific heat is given by

$$C_v = k_B \sum_j \sum_k \frac{(\frac{\hbar\omega}{2k_B T})^2}{(sinh\frac{\hbar\omega}{2k_B T})^2} \tag{164}$$

Where j stands for longitudinal, bending, and torsional branches and $\omega(k)$ can be obtained from the dispersion relations of the modes. In order to find Debye Temperature Θ_D we write:

$$k_B \sum_j \sum_k \frac{(\frac{\hbar\omega}{2k_B T})^2}{(sinh\frac{\hbar\omega}{2k_B T})^2} = \frac{RL}{6rN_c} (\frac{1}{v_L^2}+\frac{1}{v_T^2}) \frac{k_B^3 T^2}{\hbar^2} \int_0^{\frac{\Theta_D}{T}} \frac{x^3 e^x}{(e^x-1)^2} \, \mathrm{d}x + \frac{R^3 L^3}{6\sqrt{2}\pi^2 rN_c} \frac{1}{v_B^3} \frac{k_B^4 T^3}{\hbar^3} \int_0^{\frac{\Theta_D}{T}} \frac{x^4 e^x}{(e^x-1)^2} \, \mathrm{d}x$$

And we solve for Θ_D at each temperature.

3. Derivation of the Mode Grüneisen Parameter as a function of temperature

The Grüneisen parameter γ describes how the volume change of a crystal affects the vibrational properties. It can be determined as a function of temperature by using the following formula:

$$\gamma = \frac{\sum_j \sum_k \gamma_j (k) C_v(k)}{\sum_k C_v(k)} \tag{165}$$

where $\gamma_j(k) = \frac{-\Omega}{\omega(k)} \frac{\partial \omega_j(k)}{\partial \Omega}$

Where Ω is the volume of the nanowire under study.

Since $\omega_L{}^2 = \frac{E}{\rho} \pi^2 [(\frac{z_m}{\pi R})^2 + (\frac{n_3}{L})^2]$ and since the volume change of the nanowire is due to both changes in both length and the cross-sectional area of the nanowire, we can write

65

$$\gamma_L(k) = \frac{-L}{\omega_j(k)} \frac{\partial \omega_L(k)}{\partial L} \times \frac{-\pi R^2}{\omega_L(k)} \frac{\partial \omega_L(k)}{\partial(\pi R^2)}$$

$$= \left(\left(\sqrt{\frac{E}{\rho}}\right)^2 \frac{\pi^2 n_3{}^2}{L^2 \omega_L^2(k)} \right) \times \left(\left(\sqrt{\frac{E}{\rho}}\right)^2 \frac{z_m^2}{2R^2 \omega_L^2(k)} \right) \tag{166}$$

Using a similar approach,

$$\gamma_T(k) = \left(\left(\sqrt{\frac{C}{\rho I}}\right)^2 \frac{\pi^2 n_3{}^2}{L^2 \omega_L^2(k)} \right) \times \left(\left(\sqrt{\frac{C}{\rho I}}\right)^2 \frac{z_m^2}{2R^2 \omega_L^2(k)} \right) \tag{167}$$

With respect to the bending mode

$$\omega_B{}^2 = \frac{E I_{x,y}}{\rho S} \pi^4 \left[\left(\frac{z_m}{\pi R}\right)^2 + \left(\frac{n_3}{L}\right)^2 \right]^2$$

$$\gamma_B(k) = \frac{-L}{\omega_B(k)} \frac{\partial \omega_B(k)}{\partial L} \times \frac{-\pi R^2}{\omega_B(k)} \frac{\partial \omega_B(k)}{\partial(\pi R^2)}$$

$$= \left[\frac{2 E I \pi^4}{\rho S \omega_B^2(k)} \left(\frac{z_m^2}{\pi^2 R^2} + \frac{n_3^2}{L^2} \right) \frac{n_3^2}{L^2} \right] \left[\frac{E I \pi^2}{\rho S \omega_B^2(k)} \left(\frac{z_m^2}{\pi^2 R^2} + \frac{n_3^2}{L^2} \right) \frac{z_m^2}{R^2} \right] \tag{168}$$

At this point, the overall Grüneisen parameter γ can be obtained.

CHAPTER VI

RESULTS

In chapters 4 and 5, we have developed a predictable model for the lattice thermal conductivity in pristine and cylindrical nanowires respectively. Boundary scattering rates, induced by the low-dimensionality of the materials, have been derived along with the appropriate modification of the phonon dispersion relations due to phonon confinement. The formalism for the lattice thermal conductivity is formulated following Callaway's procedure. Crystal vibrational parameters including specific heat, Debye temperature and Grüneisen parameter are derived.

Using this approach, we have computed using MATLAB the thermal conductivity of silicon cylindrical and pristine nanowires using silicon bulk values as parameters to predict properties of nanowires. The integrals were calculated using Simpson's quadrature method. The predictions from our model were compared to experimental values reported on these structures.

Shown in figure 5 are the measured thermal conductivities for Si nanowires of different diameters (22, 37, 56, and 115 nm) in comparison to the thermal conductivity of bulk Si. It can be seen that the thermal conductivities are about two orders of magnitude lower than that of bulk silicon which is bell-shaped. And the figure shows that as the wire diameter is decreased, the corresponding thermal conductivity is reduced [24]. The predictions for silicon cylindrical nanowire as predicted by our model is shown in figure 6 compared to experimental data reported by Li and co-workers [24].

A strong agreement with experimental values is reached within our framework which does not contain any adjustable parameter except the specularity factor which varies from one surface to another according to its asperities and roughness.
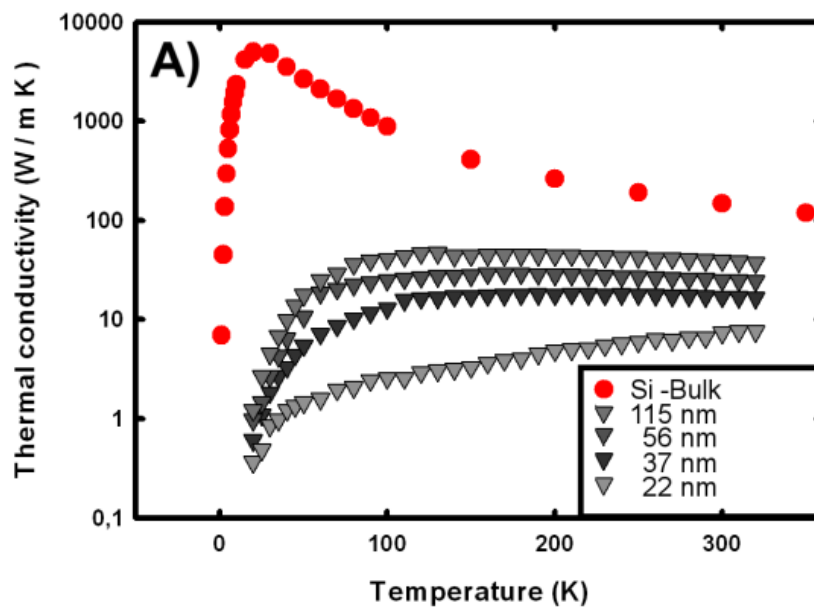

Figure 5: Thermal conductivity of bulk silicon versus that of nanowires with different diameters
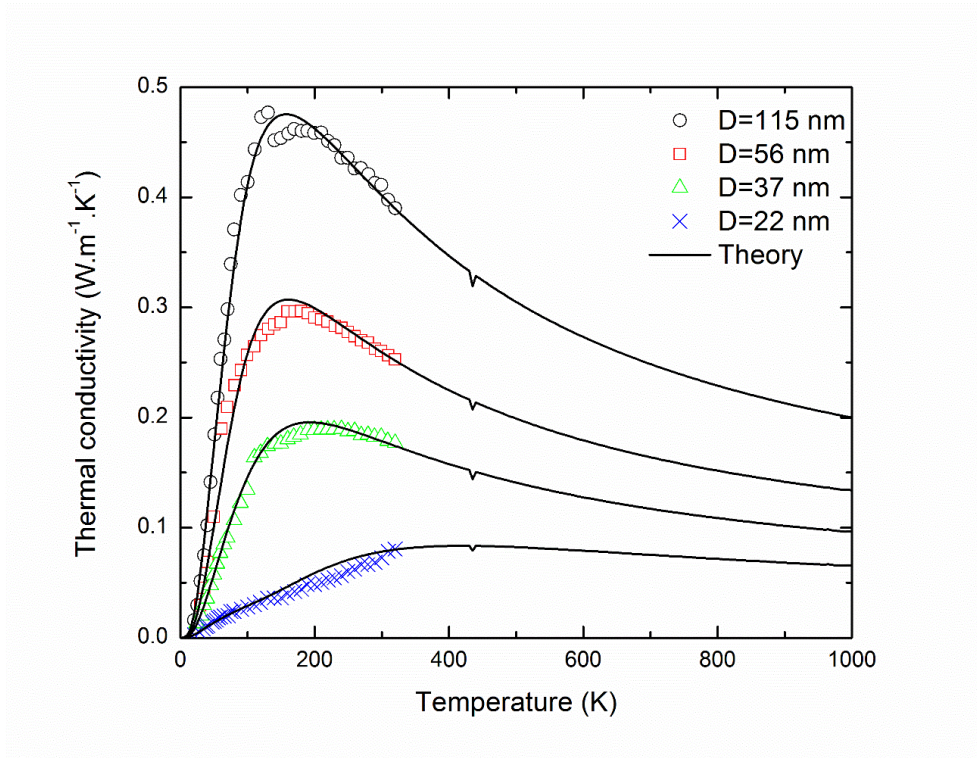
Figure 6: Plot of the predicted and measured thermal conductivity of different diameter Si nanowires.

The reduction in the thermal conductivity indicates the effect of boundary scattering on the transport of phonons in the silicon nanowires. The nanowires with diameters 37, 56 and 115 nm have thermal conductivities with peak values around 210, 160, and 130K, respectively. On the other hand, the thermal conductivity of bulk silicon reaches its peak at around 25K. The shift of the thermal conductivity peak indicates that as the diameter of the nanowire is reduced the phonon-boundary scattering process dominates over the resistive umklapp scattering mechanism, which is in turn responsible of the decrease in the lattice thermal conductivity at high temperatures. An exception here for the 22 nm diameter nanowire that does not show a peak. An additional important feature is the temperature dependence of the nanowires' thermal conductivities at low temperatures. The thermal conductivity data of 115 and 56 nm

diameter nanowires exhibits a T^3 dependence mirroring the specific heat behavior. As the nanowire diameter is reduced, the thermal conductivity of 37 nm wire deviates from T^3 to T^2 dependence and the 22 nm wire shows a linear temperature dependence of K. The 22 nm wire values could be explained by some other effects at this small scale.

In what follows, we are interested to show our model results of the thermal conductivities of pristine nanowires with different length sides. A comparison is presented through figure 7 between the data for cylindrical versus pristine nanowires. Note here that in both cases, cylindrical and pristine nanowires, the only adjustable parameter is the specularity factor and is taken to be equal to 0.5.
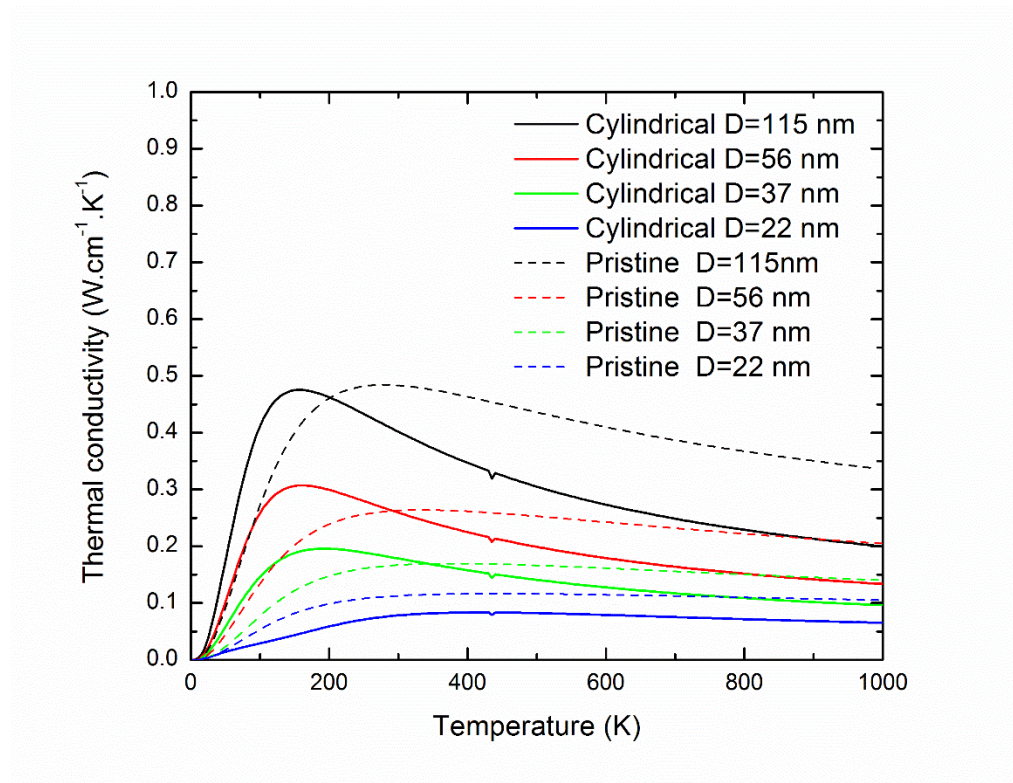

Figure 7: Thermal conductivities of cylindrical and pristine nanowires with different cross-section dimensions.

As for the case of cylindrical nanowires, pristine nanowires curve deviates from the bell-shape and shows a reduction in the lattice thermal conductivity. Similarly, as the nanowire cross-section length side decreases, the corresponding thermal conductivity reduces. As for comparison with cylindrical nanowires, the 115 nm diameter cylindrical nanowire shows a higher thermal conductivity than the pristine nanowire below a temperature around 200K. In the region above 200K, pristine nanowires show a higher thermal conductivity instead. Same results for 56 and 37 nm diameter cylindrical wires and pristine ones are found but with a shift in the inflection temperature point. The thermal conductivities for pristine nanowires indicate from the figure peak values at higher temperatures than the cylindrical nanowire. This can be explained by the presence of boundary scattering process in pristine nanowires for a wider temperature range due to the edges of the cross-section that enhance boundary scattering.

CHAPTER VII

SUMMARY AND FUTURE WORKS

A. Conclusions

The thesis was mainly devoted to develop a theoretical predictable model to find the lattice thermal conductivity in cylindrical and pristine nanowires. The approach involves analytical solution by Boltzmann Transport Equation with the relaxation time approximation following Callaway's procedure to derive the lattice thermal conductivity expression. Phonon confinement effects and low-dimensionality allow the modification of the phonon dispersion relations. Phonon transport is described along three modes: longitudinal, torsional and bending branches. Allowable normal modes have been found in cartesian and cylindrical coordinates to describe the allowable wave vectors in pristine and cylindrical nanowires. Boundary scattering relaxation times have been derived in both cases and studied in terms of the specularity factor p. Crystal vibrational parameters such as Debye temperature and Grünesien parameter are calculated. Comparison with experimental values for silicon nanowires revealed a strong agreement with the calculated values that we reported from our model. A good knowledge concerning the difference in thermal conductivities of cylindrical and pristine nanowires is presented.

B. Future Work

This model in hand is expected to predict the lattice thermal conductivity for nanotubes taking into consideration modifications to the normal modes and corresponding boundary conditions imposed on the problem. This topic will be studied.

BIBLIOGRAPHY

[1] Gang Chen. Nanoscale Energy Transport and Conversion: a parallel treatment of electrons, molecules, phonons and photons. January, 2005.

[2] C. L. Tien and G. Chen, Trans. ASME, Journal of Heat Transfer, 116, 799 (1994).

[3] Ankit Jain. Thermal Transport in Semiconductors and Metals from first-principles. PhD thesis, Carnegie Mellon University, 2015.

[4] G. Chen, D. Borca-Tasciuc, and R. G. Yang. Nanoscale Heat Transfer. Encyclopedia of Nano-science and Nanotechnology. 2004

[5] K. E. Goodson and Y.S. Ju, Annual Review of Materials Science, 29, 261 (1991).

[6] G. Chen. Annual Review of Heat Transfer, 7, 69 (1996).

[7] T. Tritt. Recent Trends in Thermoelectric Materials Research. Semiconductors and Semimetals Series, Vol. 69-71. Academic Press, San Diego, 2001.

[8] G. Chen and A. Shakouri, Trans. ASME, Journal of Heat Transfer, 124, 242 (2002).

[9] Joseph Callaway. Model for lattice thermal conductivity. Physical Review, 113(4), February 1959.

[10] M.G.Holland. Analysis of lattice thermal conductivity. Physical Review, 132(6), December 1963.

[11] M. Asen-Palmer, K. Bartkowski, E. Gmelin, and M. Cardona et al. Thermal conductivity of germanium crystals with different isotopic compositions. Physical Review B, 56(15), 1997.

[12] D.T.Morelli and J.P.Heremans. Estimation of the isotope effect on the lattice

thermal conductivity of group iv and group iii-v semiconductors. Physical Review B, 66, 2002.

[13] N.W. Ashcroft and N.D. Mermin. Solid state physics. Saunders College, 1976.

[14] Zeinab Alameh. New Model for Thermal Conductivity across Boundaries. MS thesis, American University of Beirut, 2012.

[15] H.B. Casimir. Note on the conduction of heat in crystals. Physica 5, 6, 1938.

[16] P.G. Klemens, Proc. Roy. Soc. (London) A208, 108 (1951).

[17] Herring. Physics Review, 95, 954 (1954).

[18] I. Pomeranchuk, Journal of Physics (Moscow) 5, 237 (1942).

[19] T. H. Geballe and G. W. Hull. Physics Review, 110, 773 (1958).

[20] G. Leibfried and E. Schlomann. Nachr. Akad. Wiss. Gottingen, IIa(4), 71 (1954).

[21] G. H. Zhu, H. Lee, Y. C. Lan, X. W. Wang, G. Joshi, D. Z. Wang, J. Yang, D. Vashaee, H. Guilbert, A. Pillitteri, M. S. Dresselhaus, G. Chen, and Z. F. Ren. Increased Phonon Scattering by Nanograins and Point Defects in Nanostructured Silicon with a Low Concentration of Germanuim. Physics Review Letters 102, 196803 (2009).

[22] X. W. Wang, H. Lee, Y. C. Lan, G. H. Zhu, G. Joshi, D. Z. Wang, J. Yang, A. J. Muto, M. Y. Tang, J. Klatsky, S. Song, M. S. Dresselhaus, G. Chen, and Z. F. Ren. Enhanced thermoelectric figure of Merit in nanostructured n-type silicon germanium bulk alloy. Applied Physics Letters **93**, 193121 (2008).

[23] T.Ruf, R.W. Henn, M. Asen-Palmer, E. Gmelin, M. Cardona, H.J. Pohl, G.G. Devyatych, and P.G. Sennikov. Thermal conductivity of isotopically enriched Si. Applied Physics Letters 115 (2000).

[24] Deyu Li, Yiying Wu, Philip Kim, Li Shi, Peidong Yang and Arun Majumdar. Thernal Conductivity of individual silicon nanowires. Applied Physics Letters, Vol. 83, 14 (2003).

[25] L.H. Liang and Baowen Li. Size-dependent thermal conductivity of nanoscale semiconducting systems. Physical Review B, 73, 2006 (2006).

[26] Natalio Mingo, Liu Yang, Deyu Li and Arun Majmudar. Predicting the thermal conductivity of Si and Ge Nanowires. Nano-Letters, Vol. 3, No. 12 (2003).

[27] Mei-Jiau Huang, Wen-Yen Chong, and Tai-Ming Chang. The lattice thermal conductivity of a semiconductor nanowire. Journal of Applied Physics 99, 114318 (2006).

[28] Hochbaum AI, Chen R, Delgado RD, Liang W, Garnett EC, Najarian M, Majumdar A, Yang P. Enhanced thermoelectric performance of rough silicon nanowires. Nature London 45, 163 (2008).

[29] M. Kazan, G. Guisbiers, S. Pereira, M.R. Correia, P. Masri, A. Bruyant, S. Volz, and P. Royer. Thermal conductivity of silicon bulk and nanowires: Effects of isotopic composition, phonon confinement, and surface roughness. Journal of Applied Physics 107, 083503 (2010).

[30] M. Kazan and S. Volz. Calculation of the lattice thermal conductivity in granular crystals. Journal of Applied Physics 115, 7 (2014).

[31] G. P. Srivastava. The Physics of Phonons (1990).

[32] https://physicsmadeeasy.files.wordpress.com/2008/01/monatomic-chain.jpg

[33] https://physicsmadeeasy.files.wordpress.com/2008/01/dispersion-relation3.jpg

[34] http://img.tfd.com/ggse/04/gsed_0001_0012_0_img2975.png

[35] http://img.tfd.com/ggse/e4/gsed_0001_0012_0_img2976.png

[36] G. Chen, D. Borca-Tasciuc, and R. G. Yang. Nanoscale Heat Transfer.

Encyclopedia of Nano-science and Nanotechnology. 2004